Agricultural and Forest Meteorology 320 (2022) 108939

Contents lists available at ScienceDirect

Agricultural and Forest Meteorology

journal homepage: www.elsevier.com/locate/agrformet

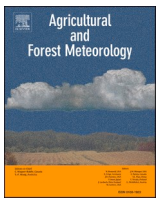

Wildfire controls on land surface properties in mixed conifer and ponderosa pine forests of Sierra Nevada and Klamath mountains, Western US

Surendra Shrestha [a,*], Christopher A. Williams [a], Brendan M. Rogers [b], John Rogan [a], Dominik Kulakowski [a]

[a] Graduate School of Geography, Clark University, Worcester, MA 01610, USA
[b] Woods Hole Research Center, Falmouth, MA 02540, USA

ARTICLE INFO

Keywords:
Wildfire
Post-fire recovery
Biogeophysical
Biochemical
MODIS
Remote sensing

ABSTRACT

This study examines the post-fire biogeophysical and biochemical dynamics after several high-severity wildfires that occurred in mixed conifer and ponderosa pine forest types in the Sierra Nevada and Klamath Mountains regions between 1986 and 2017. We found a consistent pattern of reduced leaf area index (LAI) in the first year after fire, followed by gradual recovery over the subsequent 25 years. Recovery rate varied between forest types. For example, average summer LAI for 16-25 years post-fire was 88% of the pre-fire average for mixed conifers in the Sierra Nevada, 64% for ponderosa pine in the Sierra Nevada, and 83% for mixed conifers in Klamath Mountains (63, 35, and 64% in winter, respectively). The slower recovery of LAI in ponderosa pine could be due to poor species diversity and drier climate. Summer and winter albedo increased progressively until 12 years post-fire in Sierra Nevada, while it continued to increase until 25 years post-fire in Klamath Mountains. Ponderosa pine had the highest summer (0.148 ± 0.001) and winter (0.5 ± 0.0033) albedos. Post-fire changes in evapotranspiration (ET) and gross primary productivity (GPP) were consistent with the changes in LAI. Both summer and winter ET and GPP returned to pre-fire levels by 25 years after fire in mixed conifers of both regions, while the ET and GPP did not recover to pre-fire levels in ponderosa pine. Wildfires increased the land surface temperature (LST) immediately after fire in summer. This effect was significantly higher in mixed conifers of the Sierra Nevada (11 ± 0.03 °C) compared to Klamath Mountains (7 ± 0.01 °C). Our results suggest that reduced ET, consistent with less leaf area and its associated reduced evaporative cooling is the main factor controlling the immediate post-fire warming effect of wildfires in these regions. The findings reported here can be used to understand ecological responses to wildfire in these and nearby ecoregions as they represent mean historical behavior across multiple wildfire events.

1. Introduction

The last several decades have been marked by increases in both large wildfire frequency and intensity across the western US (Westerling et al., 2006; Abatzoglou and Williams, 2016; Westerling, 2016), especially in the mountain ecoregions of California and Colorado, threatening life and property, modifying ecosystem functioning and services, and affecting climate (Ghimire et al., 2012; Dennison et al., 2014; Abatzoglou and Williams, 2016; Williams and Abatzoglou, 2016; Williams et al., 2021). In California, the area burned by wildfire increased from 0.6 million acres y^{-1} to 0.75 million acres y^{-1} from the 2000s to the 2010s. Recently, in 2020 alone, wildfire burned more than 4 million acres in California, the most since 2002 (National Interagency Fire Center, 2020). While increased burned area in the mountains of the northwestern US have been driven by climatic factors such as increasing temperature, drier summers, below average winter precipitation, and earlier spring snowmelt (Westerling et al., 2006; Morgan et al., 2008; Littell et al., 2009; Westerling, 2016), changes in other aspects of fire regime (e.g., frequency, distribution, intensity, and duration) can be more directly influenced by human-caused ignitions (Balch et al., 2017)

Abbreviations: ET, Evapotranspiration; EVI, Enhanced Vegetation Index; fPAR, Fraction of Absorbed Photosynthetically Active Radiation; GPP, Gross Primary Productivity; LAI, Leaf Area Index; LST, Land Surface Temperature; MODIS, Moderate Resolution Imaging Spectroradiometer; NBR, Normalized Burn Ratio; NDSI, Normalized Difference Snow Index; NIFC, National Interagency Fire Center.

* Corresponding author.
E-mail address: Surshrestha@clarku.edu (S. Shrestha).

https://doi.org/10.1016/j.agrformet.2022.108939
Received 8 December 2021; Received in revised form 26 March 2022; Accepted 31 March 2022
Available online 21 April 2022

and resource management decisions and actions related fire suppression beginning more than 170 years ago (Stephens et al., 2009; Hessburg et al., 2021). Wildfire events are becoming more severe than those experienced in the last two centuries (Parks and Abatzoglou, 2020) with ongoing fire suppression in some systems and the increased likelihood of climate extremes, which, together with altered post-fire climatic conditions, might already be altering the trajectories and rates of post-fire forest recovery, with the effects likely to become more pronounced in the coming decades (Rogers et al., 2011; Tepley et al., 2017; Guz et al., 2021).

Wildfire is a critical component in terrestrial and atmospheric dynamics of our Earth system (Bowman et al., 2009; Ward et al., 2012; Archibald et al., 2018; McLauchlan et al., 2020). While wildfires, like many disturbances, catalyze ecological diversity (Stevens-Rumann and Morgan, 2019), today's acceleration of disturbance regimes can profoundly alter a wide range of ecosystem characteristics such as stand structure, species composition, leaf area, canopy ecophysiology, and micro-climate (Liu et al., 2005). Disturbance-induced ecological change can have a large and long-lasting influence on ecosystem carbon fluxes (Amiro et al., 2000; Goulden et al., 2011; Ghimire et al., 2012; Williams et al., 2016), water fluxes (Chambers and Chapin, 2002; Liu et al., 2005), and energy fluxes (Liu et al., 2005; Amiro et al., 2006; Li et al., 2017; Williams et al., 2021). It takes several years, decades, or even centuries for ecosystem fluxes to return to pre-disturbance levels, and the timeline is contingent on stand structure and composition, as well as type and intensity of disturbance (Thornton et al., 2002; Dore et al., 2010). Therefore, the expected increase in the intensity and frequency of megafires and the associated long-lasting ecological effects require spatially explicit quantification of ecosystem responses to severe wildfires to assess how these events are altering terrestrial ecosystems, how they are changing surface-atmosphere exchanges, and how the associated changes influence the evolution of the climate system.

To better understand how wildfires affect the functioning of forest ecosystems, post-fire characteristics need to be monitored continuously (Masek et al., 2013). Quantification of ecological responses to wildfire events can be achieved through either direct field measurements of ecosystem properties after fire or by using remote sensing observations. Field-based observations including flux tower measurements offer a valuable approach to documenting how carbon, water, and energy balances change with disturbance and recovery process (Williams et al., 2014). Several field-based studies have summarized the effects of wildfires on land-surface fluxes (Chambers and Chapin, 2002; Jin and Roy, 2005; Amiro et al., 2006; Randerson et al., 2006; Dore et al., 2010; Ma et al., 2020). For example, Chambers et al. (2005) reported decreased net radiation over boreal ecosystem and increased net radiation over tundra ecosystem by using tower-based microclimatic and eddy covariance flux measurements to characterize net radiation between boreal and tundra forest ecosystems before and after fire. Although local-scale insights into these ecological dynamics are emerging with the continued expansion of ecological and biophysical observation networks (e.g., AmeriFlux, NEON), these observations cannot directly quantify the larger, regional impacts on weather and climate given scale issues and limited sampling (Bonan, 2008). Remote sensing can be useful to overcome these limitations through its ability to regularly observe burned areas over time over large areas (Storey et al., 2016). Remote sensing measurements of land surface properties provide a valuable means of quantifying spatial and temporal variability before and after wildfire events. Since the mid-1980s, satellite remote sensing measurements have allowed the development of novel techniques to address three different temporal fire-effects phases: pre-fire conditions, active fire characteristics, and post-fire responses (Rogan and Franklin, 2001; Lentile et al., 2006; French et al., 2008; Veraverbeke et al., 2010; Chu and Guo, 2014). Many satellite sensors are capable of detecting and assessing burned areas (Miller and Thode, 2007; Lanorte et al., 2013). In recent years, the Moderate Resolution Imaging Spectrometer (MODIS) onboard the Terra and Aqua satellites, due to its high-quality temporal and spectral resolution and the availability of continuous data since 2000, has been widely used for both active fire detection (Chuvieco et al., 2008; Giglio et al., 2010; Giglio et al., 2018; Loboda et al., 2011) and assessing changes in land surface properties in post-fire environment (O'Halloran et al., 2012; Micheletty et al., 2014; Rogers et al., 2015). For example, Jin et al. (2012) used MODIS Enhanced Vegetation Index (EVI) product (MOD13A1) (Huete et al., 2002) during 2000-2011 to study the influence of burn severity on post-fire vegetation recovery in North American boreal forests. They found that the most severe burns had the greatest reduction in summer MODIS EVI in the first year after fire which recovered to within 90%-108% of pre-fire levels by 5-8 years after fire. Similarly, O'Halloran et al. (2014) used MODIS broadband shortwave blue-sky albedo data (MCD43A, 500m spatial resolution) (Schaaf et al., 2002) combined with field surveys of vegetation after fire in the Oregon Cascade Range to examine the hypothesis that snag attrition exerts a significant control on albedo in addition to vegetation recovery following fire. This study reported strongest correlations between albedo perturbations and vegetation densities with snags.

Most landscape-scale information, to date, on ecological impacts of wildfires comes from chronosequence studies of land surface properties in post-fire environments using multi-spectral satellite data, coupled with field data with a focus on Mediterranean (Veraverbeke et al., 2012a, 2012b; Meng et al., 2014; Yang et al., 2017) and boreal ecosystems (Amiro et al., 2000; Chambers and Chapin, 2002; Randerson et al., 2006; Lyons et al., 2008; Amiro et al., 2010; Jin et al., 2012; Rogers et al., 2013); other forest types have been less studied with only a few studies focusing on mixed conifers and ponderosa pine of western US (Chen et al., 2011; Dore et al., 2012; Meng et al., 2015; Roche et al., 2018). Moreover, most previous studies have tended to focus on individual fires and land surface components, thus providing only a partial characterization of the surface states and fluxes after fire. To our knowledge, no study has documented patterns of LAI, albedo, LST, ET, and GPP dynamics as they unfold after severe wildfire events across forest types and eco-climatic settings over large areas using satellite data, especially in the mountain ecoregions of western US. The current study aims to broaden the investigation of post-fire ecological effects and recovery patterns through application of MODIS land-surface products to a series of wildfires that occurred between 1986 and 2017 in the Sierra Nevada and Klamath Mountains. Specifically, the goals of this study were to evaluate the post-fire vegetation recovery processes over time using MODIS-derived LAI, quantify post-fire changes in surface states and fluxes based on forest types, ecoclimatic setting, snow-cover condition, and year since burn, and examine relationships between LAI and other land surface properties in these post-fire environments.

2. Methods

2.1. Study area

We focused our study in the Sierra Nevada and Klamath Mountains regions of the western US, areas that are severely disturbed by wildfires in recent decades. We considered the footprints of 409 wildfires that occurred in the study area from 1986 to 2017 (Fig. 1). Both regions contain a wide diversity of bioclimatic gradients, forest types, and disturbance regimes. The climate of California is Mediterranean, with cool-wet winters followed by a long summer drought, which creates conditions conducive to wildfires (Westerling et al., 2006). California's Sierra Nevada climate varies with elevation and latitude, as well as with a strong rain shadow effect that leads to wetter conditions on the western side of the mountain chain. Sierra Nevada forests are home to diverse range of forest species (North, 2012). Vegetation in the Sierra Nevada ranges from grassland and oak savannah at lower elevations, to pine-oak forest, mixed-conifer forest (e.g., *Pinus ponderosa, Pseudotsuga menziesii, Pinus attenuate, Quercus chrysolepis, Quercus kelloggii*), and subalpine forest at higher elevations (Roche et al., 2020). The dominant

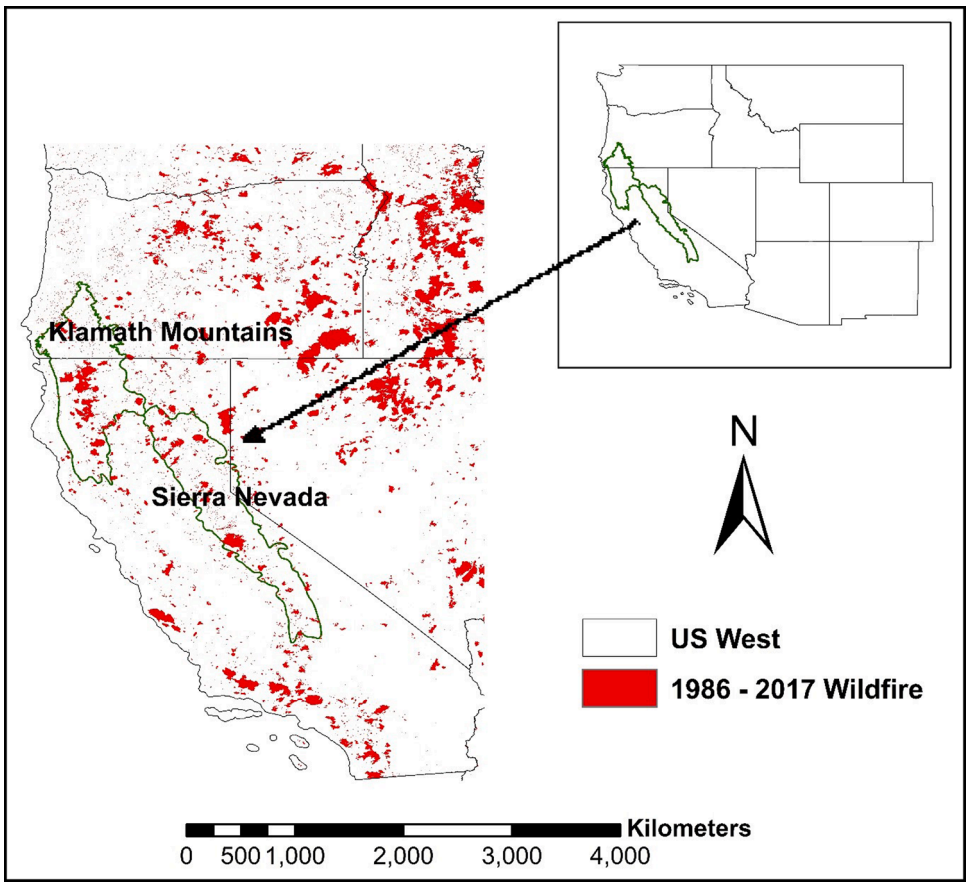

Fig. 1. Map of the Sierra Nevada and Klamath Mountains study regions within the western U.S. overlain by wildfires that burned between 1986 and 2017 (Eidenshink et al., 2007).

vegetation in Sierra Nevada is mixed conifer followed by lodgepole pine and ponderosa pine (Ruefenacht et al., 2008). The precipitation in Sierra Nevada varies with elevation, with annual precipitation ranging from 800 mm at lower elevation to more than 1700 mm at higher elevations where most precipitation occurs during the winter as snow (Lutz et al., 2009).

The Klamath Mountains is also characterized with high topographic relief and steep climatic gradient. The climate is Mediterranean, with substantial variation in precipitation with elevation and distance from the Pacific coast (Grabinski et al., 2017). The type of vegetation and fire regime in this region are influenced by both topographical and geological complexity. The Klamath Mountains is dominated by broadleaf hardwood at the lower elevation and Douglas-fir, Ponderosa pine, and mixed conifer at higher elevations (Whittaker, 1960). The dominant vegetation in Klamath Mountains is mixed conifer followed by Douglas-fir and spruce/fir/hemlock (Ruefenacht et al., 2008).

Due to insufficient availability of high severity burn samples for some forest types, we considered only mixed conifer (SN-mixed conifer) and ponderosa pine (SN-ponderosa pine) in the Sierra Nevada, and mixed conifer (KM-mixed conifer) in the Klamath Mountains to allow for comparison of post-fire ecological responses between and within two different regions.

2.2. Remote sensing data and data products

Data on burned areas and burn severity were obtained from Monitoring Trends in Burn Severity (MTBS) for the period of 1986–2017 (Eidenshink et al., 2007). Although some subjectivity can be introduced in the classification of burn severity by MTBS into low-, moderate-, and high-severity (Eidenshink et al., 2007), in general, low-severity relates to significant damage to and consumption of low vegetation and some understory shrubs or trees; moderate-severity corresponds to total damage to and consumption of understory vegetation with some overstory tree mortality; and high-severity indicates greater or complete overstory tree mortality (Keeley, 2009). We resampled the original MTBS dataset from its 30 m resolution to 500 m resolution, and only retained 500 m pixels that had at least 75% of the 30 m pixels burned to remove noise from pixels with an unclear mix of burn and unburn conditions. We ignored pixels that were burned more than once between 1986 and 2017 as such pixels can add noise to the post-fire trajectory of ecosystem properties. We stratified our analysis of post-fire recovery by forest type as defined by a USFS forest type group map (Ruefenacht et al., 2008). We retained only those pixels that had at least 75% of their forest within a single forest type according to the 250 m forest type group map. We intersected the forest type map and fire severity map to obtain pixels that were burned with high severity in each forest type, yielding 2245, 151, and 1696 pixels in SN-mixed conifer, SN-ponderosa pine, and KM-mixed conifer, respectively.

This study utilized several spatially and temporally consistent MODIS products (Table 1) to assess the biogeophysical and biogeochemical effects of fire-induced change in vegetation in the study area. We obtained all MODIS satellite data tile subsets (tiles h8v4 and h8v5) from 2000 to 2019 from the MODIS data archive (https://www.earthdata.nasa.gov/). The main advantage of using of MODIS products over reflectance values is that these products convert reflectances into biogeophysical and biogeochemical processes more usable in and comparable to other observation and modeling studies (Bright et al., 2013). The MODIS products used in this study are provided with a sinusoidal projection and each geographic data tile covers an area of approximately 1200 × 1200 km. Within each data tile, we used quality assurance (QA)

Table 1
MODIS datasets analyzed and their resolutions, temporal coverages, and sources.

Surface Property	Dataset	Resolutions	Time Span	Source
Albedo	MCD43A3	500 m; daily	2000-Present	Schaaf et al., (2002)
LST	MYD11A1	1 km; daily	2002-Present	Wan, (2008)
fPAR/LAI	MCD15A2H	500 m; 8-day	2002-Present	Myneni et al., (2002)
ET	MOD16A2	500 m; 8-day	2001-Present	Mu et al., (2011)
GPP	MOD17A2H	500 m; 8-day	2000-Present	Running et al., (2004)
Snow Cover	MOD10A1	500 m; daily	2000-Present	Salomonson and Appel, (2004)

flags to ensure that only the highest-quality values were included, removing all retrievals involving cloud cover and those flagged for low quality.

For albedo, we used the MODIS collection 6 BRDF/Albedo daily 500 m product (MCD43A3). The MODIS albedo product provides both black-sky and white-sky albedos for MODIS bands 1-7 as well as three broad bands spanning the visible, near-infrared, and the shortwave frequencies (Schaaf et al., 2002). The black sky (BSA) and white sky albedos (WSA) represent the fraction of radiation reflected by the surface under two extreme conditions. BSA represents the fraction of reflection in the absence of a diffuse component and is a function of solar zenith angle. WSA represents the fraction of reflection in the absence of a direct component when the diffuse component is isotropic (Schaaf et al., 2002). Since BSA depends on the incident solar geometry, it is intensely affected by complex terrains like those in our study area leading to biased albedo values. To partially ameliorate this bias, we examined shortwave broadband white-sky albedo for all the dates available between 2000 and 2019 as it is less sensitive to view and solar angles (Gao et al., 2005).

Data on LAI were derived from MODIS collection 6 LAI/fraction of photosynthetically active radiation (fPAR) 8-day 500 m product (MCD15A2H) (Myneni et al., 2002). The MODIS LAI algorithm includes a main look-up-table (LUT)-based procedure that exploits the spectral information contained in red and NIR bands, and a back-up algorithm that uses an empirical relationship between the Normalized difference vegetation Index (NDVI) and canopy LAI, and fPAR (Myneni et al., 2002).

Similarly, we used the MODIS version 6 GPP 8-day 500 m product (MOD17A2H) and ET 8-day 500 m product (MOD16A2), to estimate surface energy, carbon, and water cycle processes in the post-fire environment. The GPP product is based on radiation use efficiency concept (Running et al., 2004). Previous studies confirmed that there exists no consistent overestimation or underestimation in MODIS GPP compared to productivity from field-based measurements. A direct validation comparison work by Martel et al., (2005) on MOD17A2 that used 38 years of site-observation showed a high correlation and low bias ($r = 0.859 \pm 0.173$; relative error = 24%). However, MOD17 GPP still exhibits inaccuracies due to inaccuracies in input datasets like MODIS land cover, fPAR/LAI, and daily meteorological data.

The MODIS ET product (MOD16A2) is based on the Penman-Monteith equation (Mu et al., 2011). The performance of MOD16A2 has been assessed by several authors in different parts of the globe based on comparisons with flux tower measurements. A number of studies have reported an underestimation of actual ET in arid and semi-arid regions of Europe (Feng et al., 2012; Hu et al., 2015), and an improved performance in European sites located in temperate and fully humid climates (Hu et al., 2015) and forest ecosystems (Kim et al., 2012; Bhattarai et al., 2018). Another study suggests that inaccuracies in MOD16A2 are mainly due to spatial variability of input data required by retrieval algorithm and the coarseness of the Global Modeling and Assimilation Office (GMAO) climate outputs (Kim et al., 2012).

Finally, to document changes in land surface temperature resulting from wildfires, we used MODIS version 6 LST daily product (MYD11A1; Wan, 2008) produced at a spatial resolution of 1 km. The MYD11A1 algorithm uses the classification-based emissivity method to estimate the emissivity in MODIS bands 31 and 32, and then uses generalized split-window LST retrieval algorithm to generate the LST product under clear sky condition, while under cloudy sky condition, the algorithm does not retrieve LST (Wan, 2008). The accuracy of this LST product is about 1K under clear sky conditions, according to ground validation results, and could meet the accuracy requirement of most modeling applications on LST (Wan, 2014).

We stratified the sampling of albedo and LST by snow-free and snow-covered conditions based on the corresponding snow cover condition defined at a pixel level by the MODIS snow cover daily 500 m product (MOD10A1; Salomonson and Appel, 2004). The snow product uses the Normalized Difference Snow Index (NDSI) to identify snow cover. For this study, we assigned a snow-free condition when snow cover was less than 30%, and a snow-covered condition when the snow cover was greater than 75%. We chose a threshold of 30 and 75% because it maximized data quality by removing noise from pixels with an unclear mix of snow and snow-free conditions. The summer albedo and LST used in this study were snow-free, while the winter albedo was snow-covered. We did not create snow-covered summer albedo and snow-covered summer and winter LST due to insufficient sample availability within the high severity burn conditions.

2.3. Analyzing biophysical and biochemical responses to fires

MODIS estimates of LAI have shown unrealistic variation between eight-day composites in coniferous forest (Cohen et al., 2006). To control for unrealistic variation in LAI, albedo, ET, GPP, and LST, as a preliminary step in our analysis, we computed mean monthly (e.g., LAI, albedo, and LST), or total monthly (e.g., ET and GPP), values that we could later sample with time since burning (in years) by compositing all samples within our stratified design. We computed average monthly summertime values of LAI, albedo, ET, GPP, and LST for each year by adding June, July, and August grids and dividing by the number of composites in these months. Yearly winter values of these variables were computed the same way using data from December, January, and February. In the case of albedo and LST, we first sampled burned pixels based on snow-free and snow-covered conditions using the threshold mentioned above and then computed mean monthly values within those strata, separately. Initial preprocessing involved transforming spatial resolutions and projections, clipping the dataset to the appropriate locations of study, and creating associated intermediate time series data stacks of monthly maps.

We then analyzed how surface properties like albedo, LST, LAI, ET, and GPP change post-fire relative to pre-fire by sampling each product as an annual time series from pre-fire years to post-fire and analyzing for differences at least three years before wildfire events and for all years of record after wildfire events. Samples from each fire event were pooled according to strata of forest type, climate setting, and snow cover conditions and compared across these classes. Within these classes, burn events from different years were composited together and temporally aligned to represent three years prior to and all years after burning. For example, we used MODIS data products from 2001 to 2019 and therefore, the one-year post-fire composite includes pixels that were burned between 2000 and 2017 (final year of fire data) as 2001 MODIS data serves as one-year post-fire for 2000 fires, 2002 MODIS data serves as one-year post-fire for 2001 fires and so on. This enabled us to examine how satellite-derived biophysical properties vary with wildfire events. The trajectory of surface properties for mixed conifer and ponderosa pine within the Sierra Nevada region were compared to assess within-region variability, while the trajectory of mixed conifers in Sierra

Nevada and Klamath mountains were compared to assess among-region variability. In addition, changes in land surface properties were averaged within preset time-intervals of 0-5, 6-15, and >15 years post-fire, and by season. The width of the time intervals was based on the notion that there will be abrupt change in the first few years post-fire and gradual change in subsequent years. Since the directionality of post-fire albedo changes rapidly in the first few years, we further categorized 0-5 years post-fire interval into 0-3 years post-fire and 4-5 years post-fire to capture the diverse pattern of albedo perturbation post-fire. This approach generated seasonal curves for changes in surface properties that ensue with time since fire and for specific forest types and ecoregions. We calculated the group means for pre-fire and preset time-intervals and tested their difference through combining one-way analysis of variance (ANOVA) and Tukey's honest significant differences (HSD).

To detect forest type-specific anomalies in surface properties due to wildfire in the seasonal trajectory of burned sites, the seasonal differences between average pre-fire values and post-fire values for each year were calculated as:

$$\Delta X_{i,j} = X_{post-fire,i,j} - X_{pre-fire_{avg},i}$$

Where $X_{post-fire,i,j}$ is post-fire biophysical property under study for forest type i (i = SN-mixed conifer, SN-ponderosa pine, KM-mixed conifer) and post-fire year j ($j = 1, 2, \ldots, 25$) and $X_{pre-fire_{avg},i}$ is an average value of pre-fire biophysical property for forest type i. The difference metric can be used to provide insight into the post-fire ecological response to wildfire.

Pearson's correlation coefficient was used to examine variance in annual ecosystem properties explained by LAI, with statistical significance set at $\propto = 0.05$.

3. Results

3.1. Effects of wildfire on post-fire vegetation recovery

LAI values were substantially reduced by fire, with a gradual recovery toward the pre-burn LAI values, but remaining diminished even 25 years later (Fig. 2a–c). The magnitude of decline post-burn, and the rate of post-burn recovery varied by forest type. Leaf area exhibited a simple seasonal cycle in all three examples, with a mid- to late-summer peak and a winter minimum. Pre-fire LAI continued to increase through the growing season to a late season peak for mixed confers in both regions, but post-fire LAI peaked in the early summer season. For ponderosa pine stands, the seasonal timing of the peak in LAI was largely unaltered by burning. The largest difference between pre-fire and post-fire LAI occurred during the growing season (Fig. 2a–c). The increase in LAI from 0–5 years since fire to 16–25 years since fire indicates vegetative recovery over post-fire years. However, the LAI was consistently lower in post-fire years compared to pre-fire LAI for all months in each forest type. The mean LAI during both summer and winter differed significantly among pre-fire and preset time-interval groups (considered representative of the recovery trends) for all forest types; large sample sizes gave statistical tests considerable power so that even small differences were significant (Fig. 2a–c).

Turning to annual time series, we found that LAI varied little across the three pre-burn years, decreased abruptly immediately after burning, and gradually increased thereafter for all forest types. LAI did not return to the pre-fire condition by 25 years after fire. The rate of LAI recovery was slowest for SN-ponderosa pine, intermediate for SN-mixed conifer, and fastest for KM-mixed conifer during both summer and winter (Fig. 2d, f). Recovery of winter LAI was slower than for summer LAI, and recovery of ponderosa pine LAI was slower than for mixed conifers (Fig. 3d and f, Table 2). The average summer LAI for 16–25 years since fire category was 88 ± 0.8, 64 ± 1.8, and 83 ± 1.1% of the pre-fire LAI,

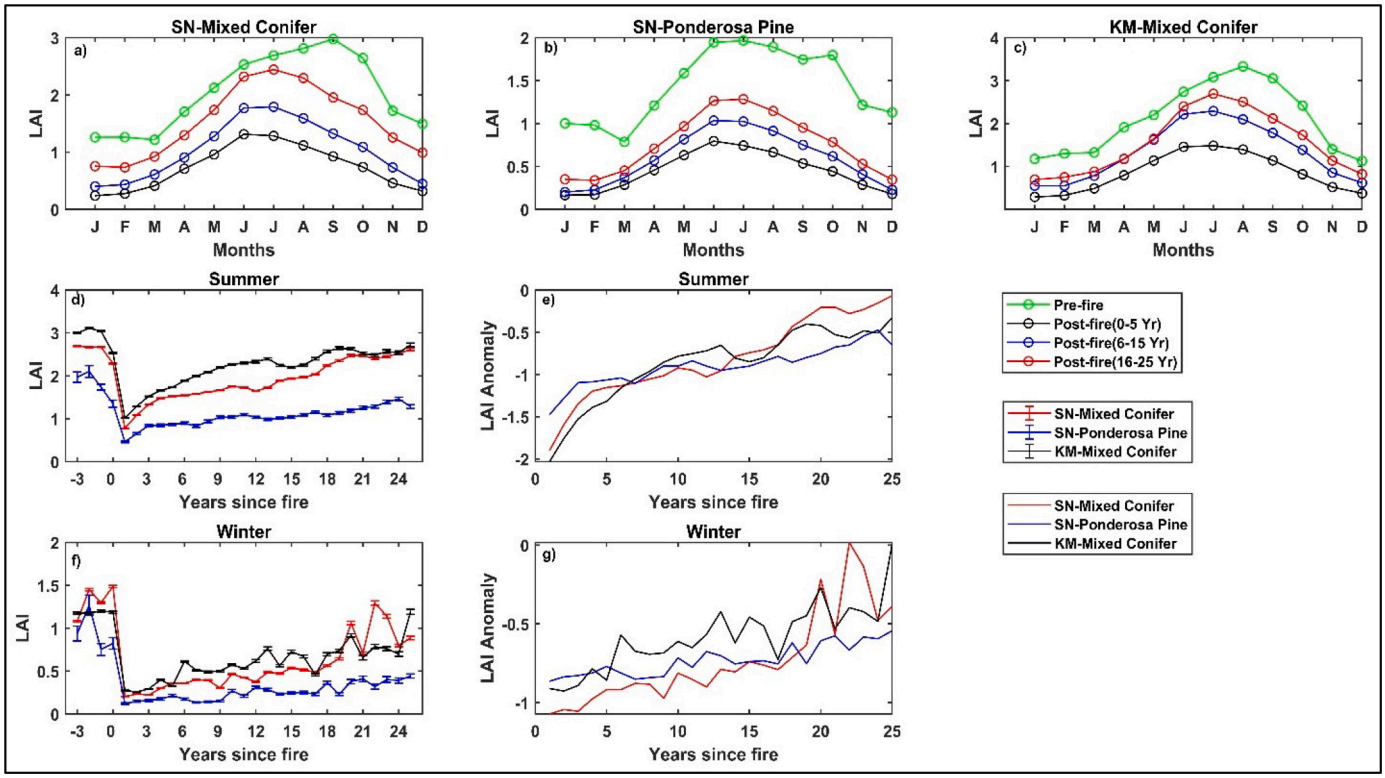

Fig. 2. Seasonal dynamics (a–c) of vegetation recovery as defined by LAI in mixed conifers and ponderosa pine forest types of Sierra Nevada and Klamath Mountains. Pre- and post-fire LAI and its anomaly during summer (d and e) and winter (f and g), where lines show means and error bars represent plus and minus one standard error.

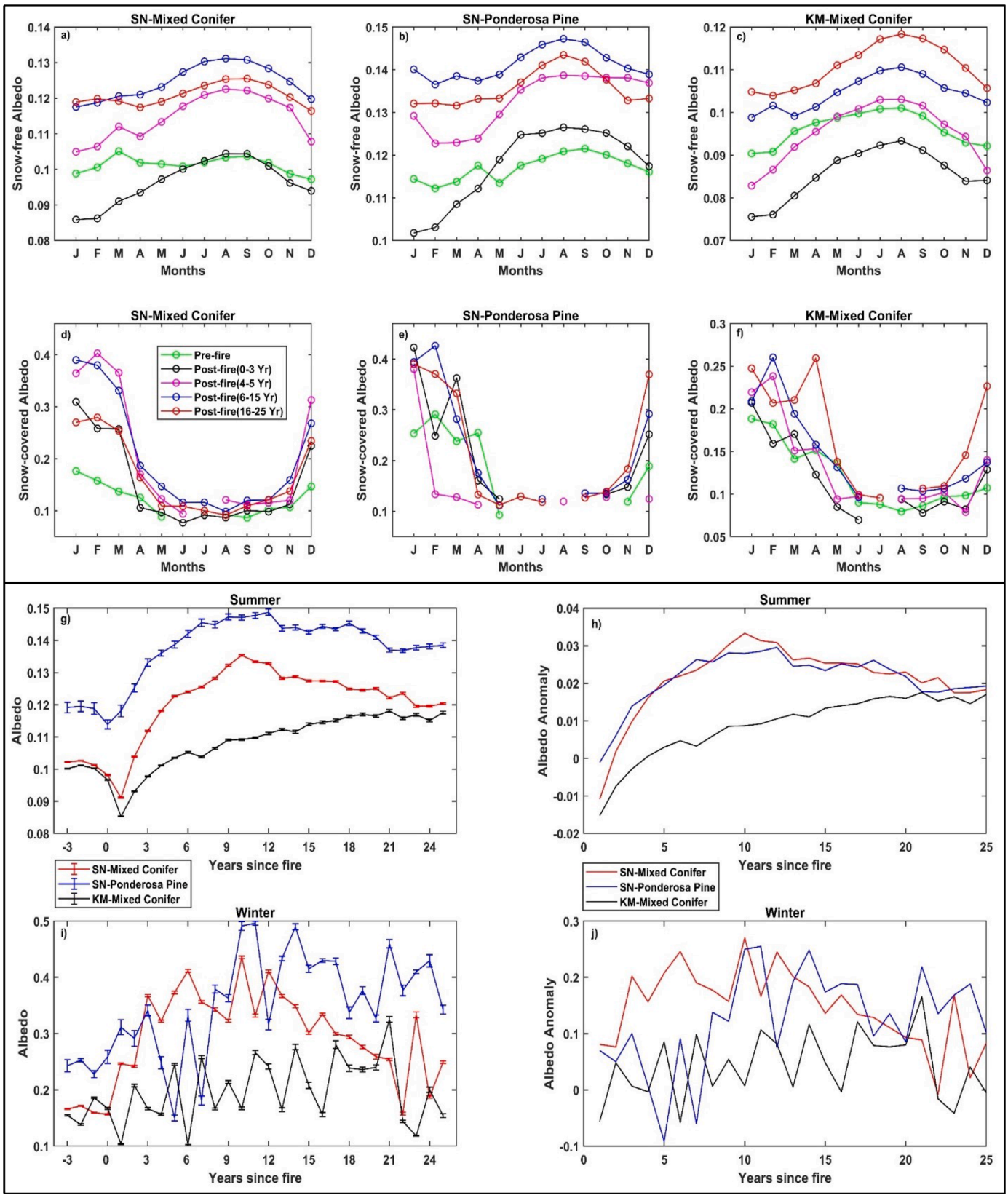

Fig. 3. Seasonal dynamics of snow-free (a–c) and snow-covered (d–f) pre-and post-fire albedo in mixed conifers and ponderosa pine forest types of Sierra Nevada and Klamath Mountains. The temporal trajectory of summer albedo (g) and its anomaly (h) represent snow-free albedo while wintertime albedo (i) and its anomaly (j) represent snow-covered albedo, where lines show means and error bars represent plus and minus one standard error.

Table 2
Average percent LAI recovery by forest type and time since fire

Average Post-fire LAI relative to pre-fire aggregated by years since burn (%)						
	Summer			Winter		
Forest Type	0 to 5 Years	6 to 15 Years	16 to 25 Years	0 to 5 Years	6 to 15 Years	16 to 25 Years
SN-mixed conifer	46 ± 0.2	64 ± 0.4	88 ± 0.8	21 ± 0.2	33 ± 0.5	63 ± 1.2
SN-ponderosa pine	38 ± 1.2	51 ± 1.2	64 ± 1.8	17 ± 1.3	22 ± 1.3	35 ± 2.5
KM-mixed conifer	47 ± 0.2	72 ± 0.6	83 ± 1.1	26 ± 0.3	50 ± 1	64 ± 1.8

for SN-mixed conifers, SN-ponderosa pine, and KM-mixed forest, respectively (63 ± 1.2, 35 ± 2.5, and 64 ± 1.8% in winter, respectively) (Table 2). The post-fire LAI of KM-mixed conifers was consistently higher than those of SN-mixed conifers and SN-ponderosa pine. The KM-mixed conifer experienced the largest difference between pre- and post-fire LAI among the forest types in the first post-fire year during summer, with a mean LAI difference of 2, while ponderosa pine experienced largest difference after 25 years since fire, with an LAI difference of 0.7 (Fig. 2e).

3.2. Effects of wildfires on surface states and fluxes

Surface albedo was substantially altered by burning, with a general increase above the pre-fire values, and with a much larger response in snow-covered winter conditions than in summer. In some cases, albedo declined in the first few years after burning. For example, we found a significant decrease in average summer snow-free albedo in the first three years after fire for mixed conifers of the Klamath region which did not recover until five years post-fire (Fig. 3c). For 0–3 years post-fire, average snow-free albedo in mixed conifer forest of both regions was consistently lower than pre-fire values during winter months (Fig. 3a–c). Time series of albedo in summer also showed an initial decline after fire, but then at about 2 or 3 years after fire, albedo was elevated above the pre-fire, typically peaking at about 12 years post-burn, while it continued to rise until year 25 post-fire in KM-mixed conifer (Fig. 3g). Elevated post-burn albedo is presumably due to increasing canopy cover, the relative high albedo of grasses and shrubs that establish in early succession, and the loss of black carbon coatings on soil and woody debris (Chambers and Chapin, 2002). Snow-covered winter albedo increased immediately after burning, though with variability in the time series of SN-ponderosa pine and KM-mixed conifers likely related to greater noise associated with smaller sample sizes. Averaged over forest types with data from multiple fire events from different years, the albedo response was more than two-fold greater in winter than in summer and peaked at an absolute albedo of 0.5 ± 0.0033 in year 11 after fire (Fig. 3i). Summer albedo remained elevated above the pre-fire level even after 25 years (Fig. 3h). Winter albedo in mixed conifers returned to pre-fire level in year 22 after fire, while it was consistently higher than pre-fire level in SN-ponderosa pine even after 25 years since fire (Fig. 3j).

The seasonal distribution of GPP was similar to that of LAI except that GPP peaked early in the growing season. GPP was much reduced in winter in all cases but rose to a peak in June for all forest types (Fig. 4a–c). The pattern of GPP post-burn was almost identical in all forest types with KM-mixed forest having highest average pre-fire (0.22 kg C m^{-2} $month^{-1}$) and post-fire (0.2 kg C m^{-2} $month^{-1}$) values among forest types (Fig. 4c). Fire had a larger effect on GPP in the summer than in other seasons. The annual time series showed sharp declines in GPP immediately after fire which then increased gradually over time. The recovery of GPP was rapid in summer than in winter owing to vegetation regrowth (Fig. 4d and f). A maximum difference of 0.075 kg C m^{-2} $month^{-1}$ occurred in SN-ponderosa pine which accounted for 65% of loss in GPP in the first year since fire (Fig. 4e). The summer and winter GPP of mixed conifer returned to the pre-fire level within 25 years after

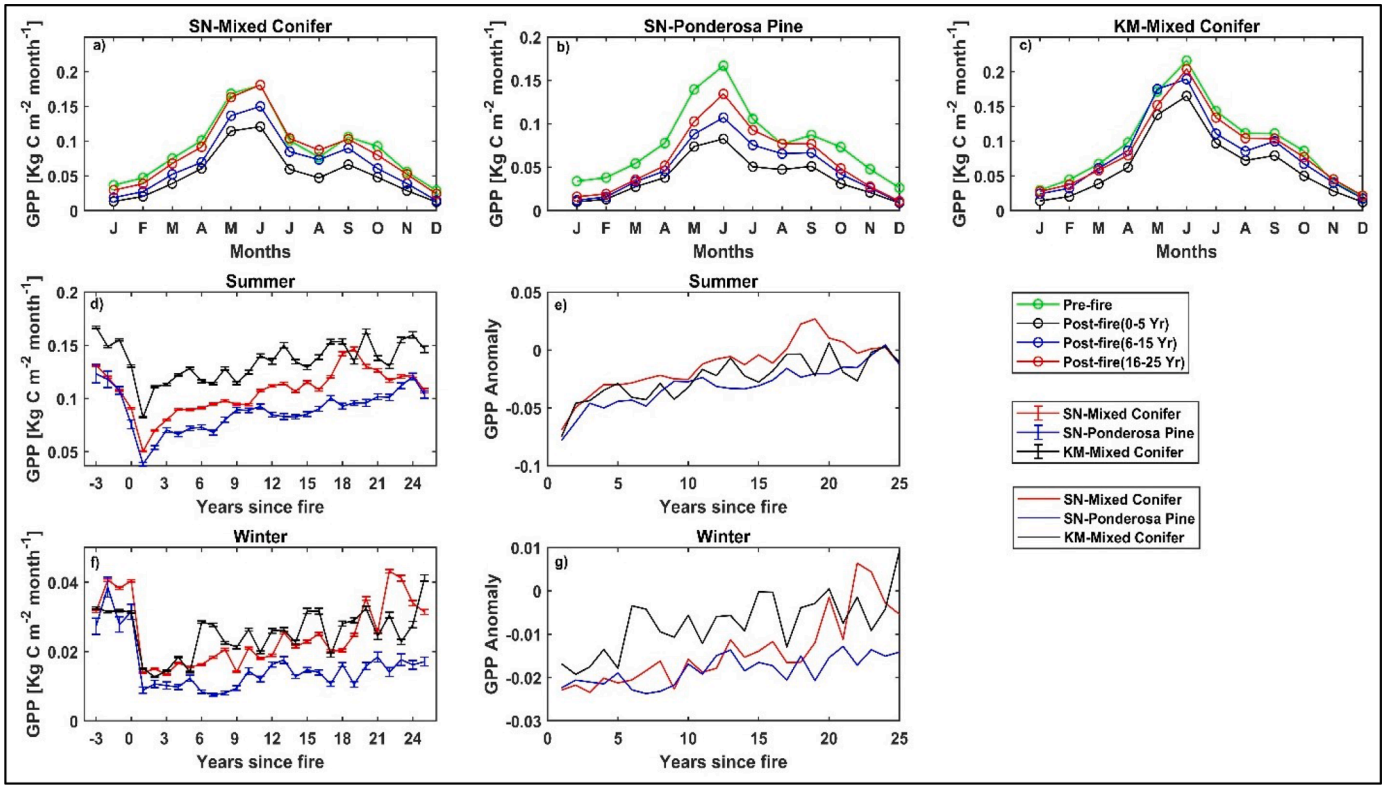

Fig. 4. Seasonal dynamics (a–c) of pre- and post-fire GPP in mixed conifers and ponderosa pine forest types of Sierra Nevada and Klamath Mountains. Pre- and post-fire GPP and its anomaly during summer (d and e) and winter (f and g), where lines show means and error bars represent plus and minus one standard error.

fire, while the winter albedo of SN-ponderosa pine was 50% below pre-fire level in year 25 after fire (Fig. 4g).

As with GPP, evapotranspiration was substantially reduced in the year immediately after fire, with a gradual recovery over two decades. The largest response was seen in summer and autumn when ET was relatively high (Fig. 5a–c). The pattern followed that of LAI, which is a key input to the MODIS ET algorithm. The declines in ET also correspond with increases in LST, which is an independent measure of land surface response and consistent with the removal of transpiring vegetation. The recovery rate of both mixed conifers was consistent until 13 years following fire, after which KM-mixed conifer trailed behind SN-mixed conifers (Fig. 5d, f). By 25 years after fire, summer and winter ET reached the pre-fire level in both mixed conifers (ET Anomaly > 0), while SN-ponderosa pine remained lower than the pre-fire ET throughout the 25-year period (ET Anomaly<0) (Fig. 5e, g).

Summer LST increased markedly 1 year after fire, with peak values of 40.5 ± 0.13 °C and 35.4 ± 0.14 °C for mixed conifers of Sierra Nevada and Klamath mountains, respectively, presumably due to the removal of overstory and understory vegetation and associated evaporative surface (Fig. 6c). LST post-fire was elevated by as much as 11 ± 0.03 °C in SN-mixed conifers to 7 ± 0.01 °C in KM-mixed conifers (Fig. 6d). As leaf area and vegetative cover recovered, the elevation of LST diminished. However, it remained consistently higher than pre-fire LST throughout the 25-year period for all three ecoclimatic settings (Fig. 6a, b).

3.3. Correlation analysis

Although the winter and summer albedo anomalies varied substantially in magnitude, they both had a similar trend throughout the post-fire years except that summer albedo declined immediately after fire. As shown above, in the 25 year time series post-fire, albedo tended to be initially lower than pre-fire, then rose above the pre-fire value, peaked and ultimately declined again toward the pre-fire values. Therefore, the correlation analysis between albedo and LAI does not uncover the trends but rather the degree to which two variables show commensurate increases or decreases (Figs. 7a, 8a). Changes in summer albedo were positively correlated with LAI for all forest types ($p < 0.05$) (Table 3). Among forest types, KM-mixed conifer showed strong significant positive correlation between LAI and albedo ($r = 0.98$, $p < 0.0001$)(Fig. 7a and Table 3). Wintertime albedo dynamics were not as clearly correlated with LAI and the relationship was statistically significant ($p < 0.05$) only for mixed conifer forest type in Sierra Nevada (Fig. 8a and Table 3).

Both ET and GPP had strong positive relationships with LAI during both summer and winter seasons, with ET and LAI ($r > 0.71$, $p < 0.0001$) and GPP and LAI ($r > 0.84$, $p < 0.0001$) for all forest type during both summer and winter (Figs. 7, 8 and Table 3). This suggest that increase in ET and GPP is partially explained by the re-establishment of young vegetation. LST increased markedly with decreased LAI in the first year after fire and decreased gradually in the following years as LAI recovered, resulting in significant negative correlation between LST and LAI for both SN-mixed conifer ($r = -0.98$, $p < 0.0001$) and KM-mixed conifer ($r = -0.89$, $p < 0.0001$) (Fig. 7d and Table 3).

4. Discussion

We described post-fire vegetation recovery using MODIS LAI time series and the associated biogeophysical responses to wildfire using MODIS albedo, ET, GPP, and LST time series for multiple fires that occurred between 1986 and 2017 in Sierra Nevada and Klamath regions of the western United States. We documented a large decline in LAI due to fire with a multi-site average LAI recovery reaching 88% in 16-25 years post-fire in SN-mixed conifer, 83% for KM-mixed conifer, but only 64% for SN-ponderosa pine (Table 2). We expect that LAI recovery

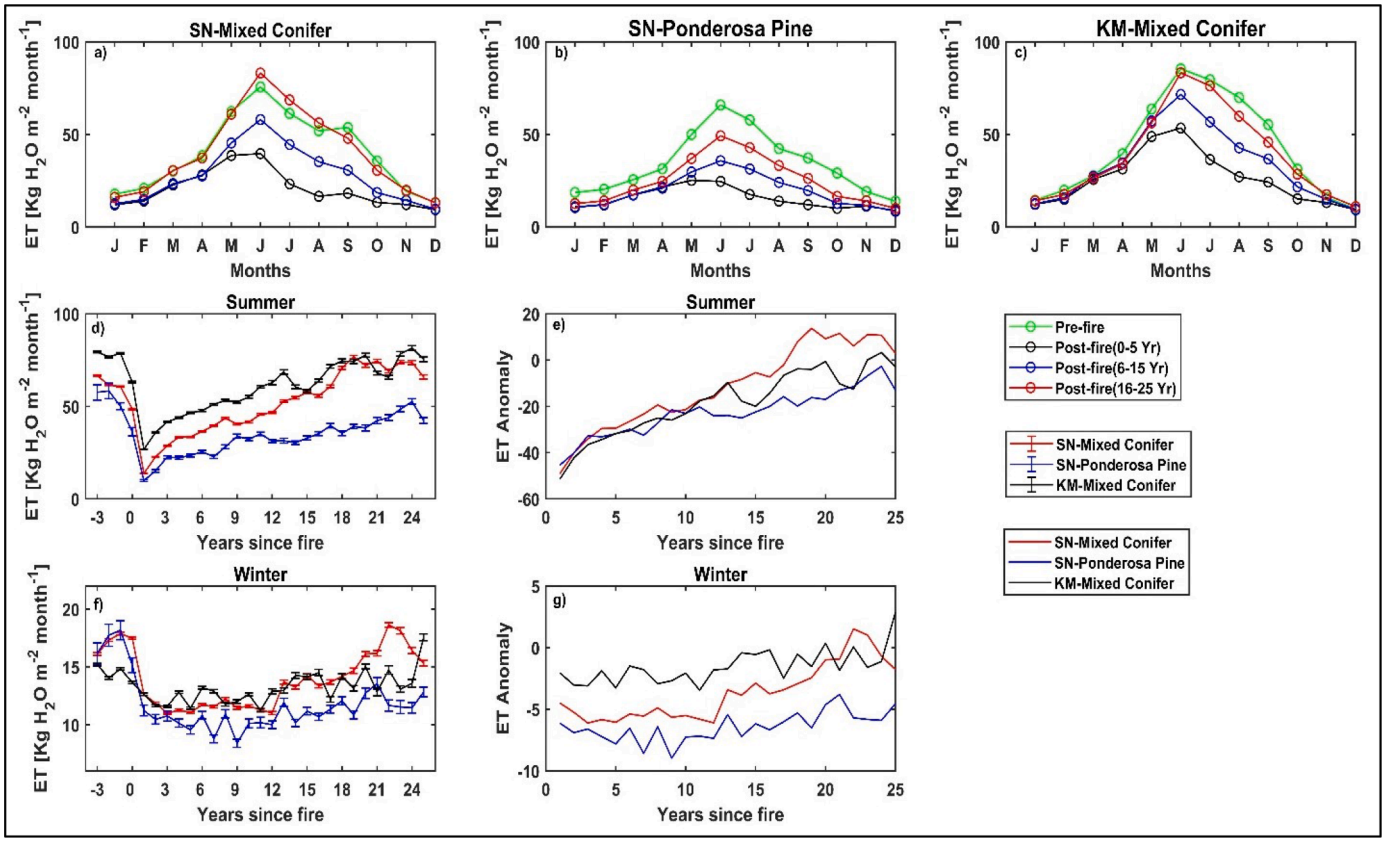

Fig. 5. Seasonal dynamics (a–c) of pre- and post-fire ET in mixed conifers and ponderosa pine forest types of Sierra Nevada and Klamath Mountains. Pre- and post-fire ET and its anomaly during summer (d and e) and winter (f and g), where lines show means and error bars represent plus and minus one standard error.

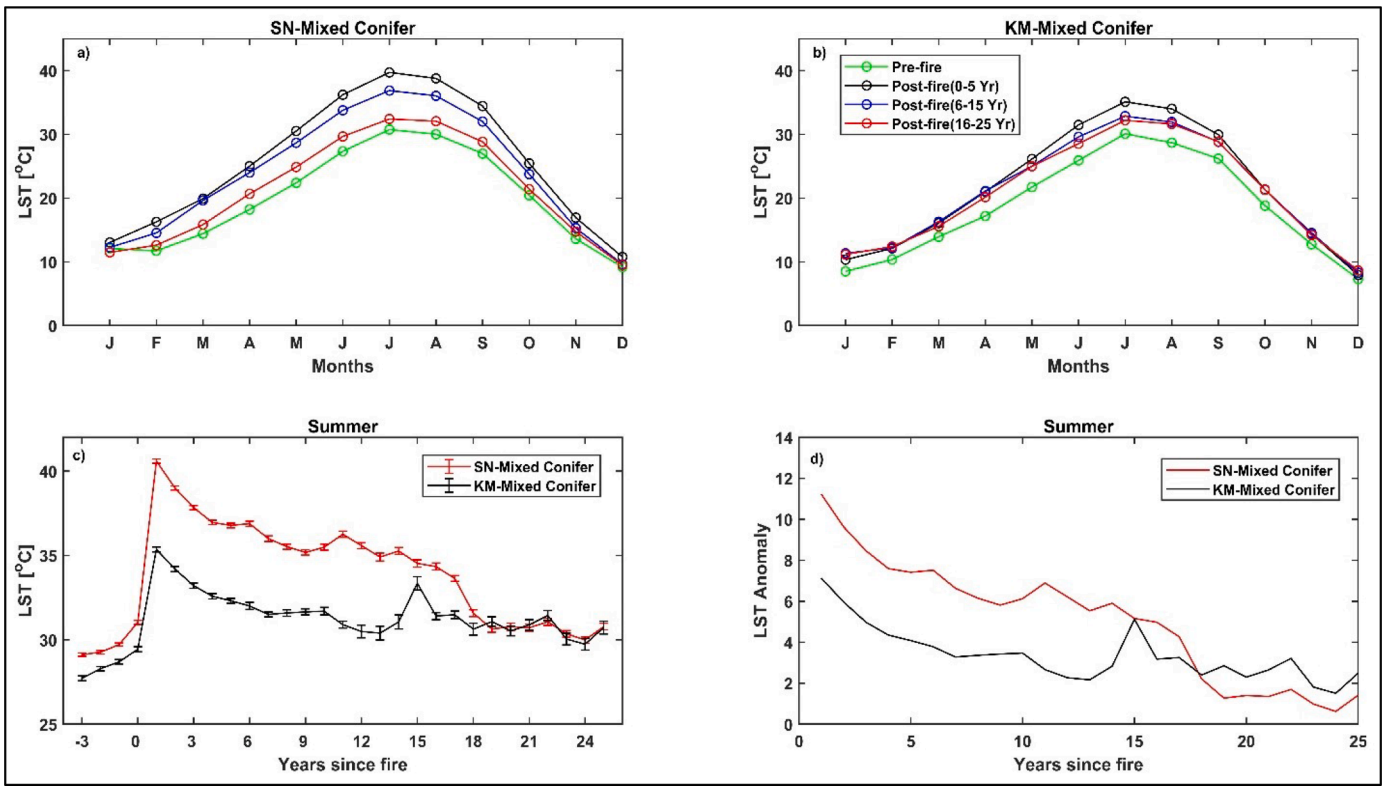

Fig. 6. Seasonal dynamics (a and b) and temporal trajectory (c and d) of pre- and post-fire LST in mixed conifers and ponderosa pine forest types of Sierra Nevada and Klamath Mountains, where lines show means and error bars represent plus and minus one standard error.

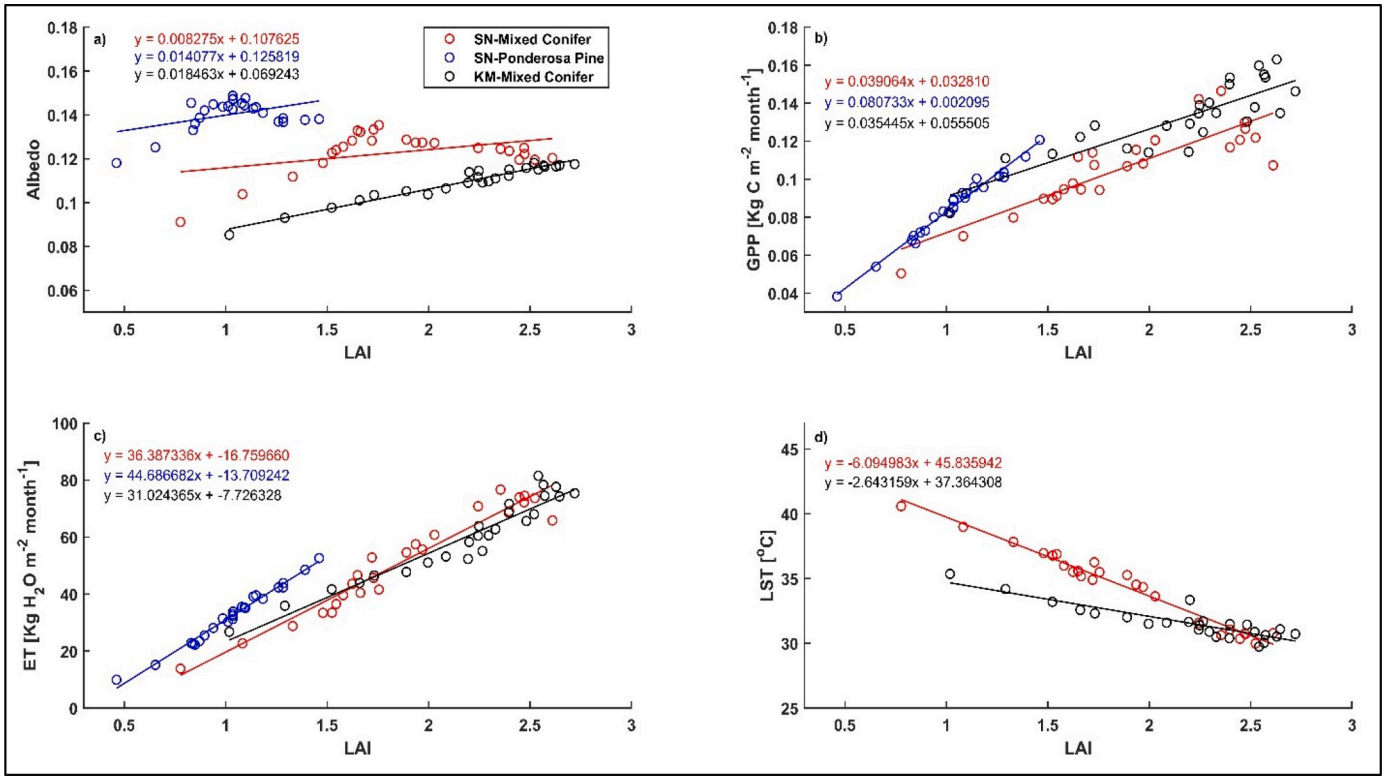

Fig. 7. Scatterplots of mean post-fire biophysical dynamics and post-fire change in LAI during summer.

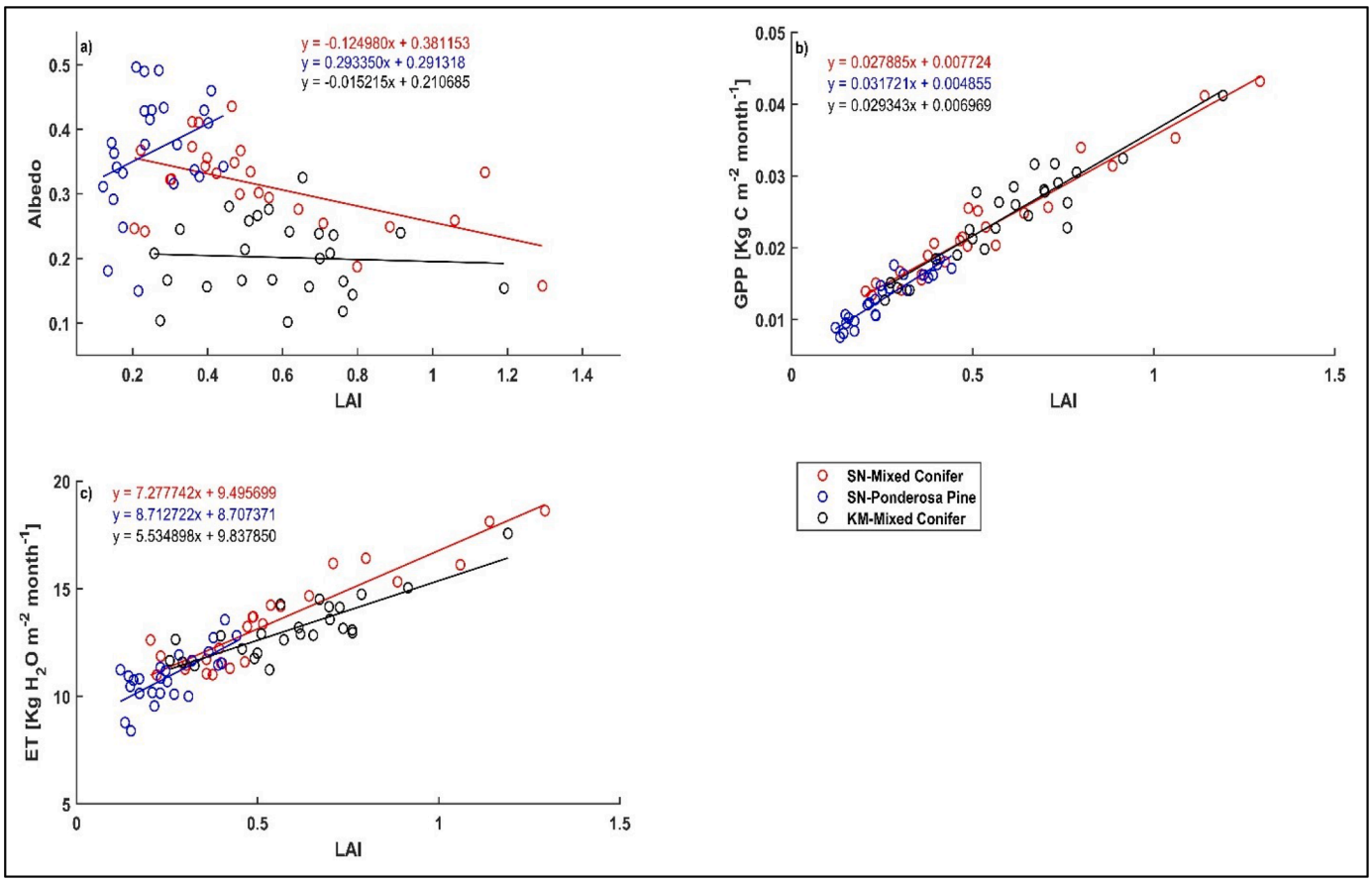

Fig. 8. Scatterplots of mean post-fire biophysical dynamics and post-fire change in LAI during winter.

Table 3
Pearson correlation coefficients between post-fire pertubation of ecosystem properties and LAI during summer and winter seasons. (Forest Types: SN_MC = Sierra Nevada mixed conifer; SN_PP = Sierra Nevada ponderosa pine; KM_MC = Klamath Mountains mixed conifer).

Surface Properties	Summer			Winter		
	SN_MC	SN_PP	KM_MC	SN_MC	SN_PP	KM_MC
Albedo	0.42***	0.44***	0.98*	-0.53**	0.32	-0.05
GPP	0.86*	0.99*	0.84*	0.97*	0.91*	0.92*
ET	0.97*	0.99*	0.95*	0.93*	0.71*	0.84*
LST	-0.98*		-0.89*			

* significant at 0.0001,
** significant at 0.01,
*** significant at 0.05

to the pre-fire state continues to unfold over time beyond the 25-year period of observation available for this study. This pattern of vegetation recovery is in agreement with the recent synthesis by Bright et al. (2019) showing the post-fire recovery of Landsat Normalized Burn Ratio (NBR). Their study arrayed data from 12 wildfires that occurred between 2000 and 2007 in three different forest types of western North America by each forest type's time since disturbance to study the temporal trajectory of vegetation recovery following wildfire disturbances. They reported consistently higher NBR recovery of mixed conifers compared to ponderosa pine with average recovery of 68% and 54% in year 13 after fire for mixed conifer and ponderosa pine, respectively. Other existing studies in different ecosystem types have reported similar or faster recovery, for example, Viedma et al. (1997) for a Mediterranean ecosystem with mean recovery time of 1 to 18 years, Epting and Verbyla (2005) for a Boreal (Alaska) ecosystem with mean recovery time of 8 to 14 years, and Hope at al. (2007) for a Chaparral (California) ecosystem with mean recovery time of 10 years. Existing studies in these regions have reported that the variation in post-fire vegetation recovery is strongly related to pos-fire climate (Meng et al., 2015; Bright et al., 2019) as temperate forests of western North America are limited by summer precipitation and cold temperatures (Nemani et al., 2003). In addition, more rapid post-fire recovery in mixed conifer compared to ponderosa pine forests could be possibly due to richer species diversity and also because mixed conifers tend to exist in a wetter climate (Bright et al., 2019). In addition, the regeneration of ponderosa pine could be impacted by secondary factors like competition with other species. For example, in a post-fire regeneration study of ponderosa pine in Arizona, Stoddarrd et al. (2018) reported absence of ponderosa pine seedlings and dominance of aspen sprouts 15 years after fire in both low- and high-severity plots as the harsh post-fire climatic condition favors aspen establishment. In year 16, ponderosa pine seedlings were found on one (13%) medium-severity plot. Such a continued lack of conifer regeneration may, with time, lead to the novel ecological conditions (Stoddarrd et al., 2018). Likewise, the faster recovery rate of mixed conifers in Klamath Mountains than in Sierra Nevada (Fig. 2d, f) might have been due to greater post-fire precipitation as it lies further north-west of Sierra Nevada and in closer proximity to Pacific Ocean.

Post-fire vegetation growth significantly affected the LAI, reflecting an alteration of carbon, water, and energy balance. Our post-fire analysis supports previous findings that post-fire albedo increases with time since fire (Montes-Helu et al., 2009; Gleason et al., 2019). Here we observed an immediate post-fire decrease in summer albedo which is consistent with previously published findings that report albedo drops in the range of 0.01–0.05 (Beringer et al., 2003; Jin and Roy, 2005; Amiro et al., 2006; Randerson et al., 2006; Lyons et al., 2008; Veraverbeke et al., 2012b). Lyons et al., (2008) and Randerson et al., (2006), based on

MODIS imageries, observed a slight decrease in summer albedo (~ 0.012), whereas Jin and Roy (2005) and Veraverbeke et al. (2012b) reported the average summer albedo drop of 0.024 and 0.032, respectively which closely approximates our values. The main reason for the immediate post-fire decrease in albedo is the large-scale replacement of living vegetation with black carbon on soil surfaces and on dead boles. The charred surface strongly absorbs the incoming solar radiation causing a significant reduction of the reflection-to-incoming sunlight ratio (Veraverbeke et al., 2012b). Additionally, the initial decline in summer albedo can also be attributed to post-fire increase in soil water content, consistent with observed decrease in ET (Montes-Helu et al., 2009). As the soil water content increases, the albedo decreases due to darkening of soil (Domingo et al., 2000) and an increase in understory leaf area in wet season (Thompson et al., 2004) based on results from other ecosystem types. Both mixed conifer and ponderosa pine showed a consistent but modest increase in summer albedo until 12 years post-fire, probably from increased grass and shrub cover and partial loss of black carbon that initially coated soil surfaces and dead boles. The increase in winter albedo in both mixed conifers and ponderosa pine in response to wildfire was likely due to increased snow exposure associated with tree mortality and loss of canopy. Our findings regarding maximum changes in snow-covered winter albedo were quite similar to those documented by Gleason et al. (2019), who documented an increase in snow-covered winter albedo by 0.31 at 13 years post-fire in western US burned forests. However, the SNICAR-modeled snow-covered winter albedo change (0.06) by Gleason et al. (2019), attributed to the deposit of black carbon on snow, was substantially lower than what we report here from empirical study. We can also compare the albedo impact of forest fires to the impact of mountain pine beetle attacks, another disturbance type common to mountainous ecosystem of the western US. Our finding of post-fire summer albedo is consistent with a small increase in summer albedo following bark beetle attack reported by O-Halloran et al. (2012) and Vanderhoof et al. (2014). Unlike after fire, where winter albedo consistently increased with time in the first 12 post-fire years, winter albedo significantly increased by 4 years after beetle attack due to loss of needles followed by decrease in albedo for about 9 years after attack due to initial release of surviving and understory trees and subsequent increase in albedo until 12 years after attack as fine branches and the smallest snags began to fall (O-Halloran et al., 2012). In regard to the role of forest type, both mixed conifers and ponderosa pine showed similar seasonal response to wildfire; however, SN-ponderosa pine showed substantially higher winter and spring albedos in 16–25 years post-fire (Fig. 3a–f), compared to SN-mixed conifer. This difference may be attributed to slower post-fire recovery of ponderosa pine (Bright et al., 2019) which is characterized by a more open canopy for a longer period of time, and which in turn elevates illumination of the ground's snow cover which is highly reflective.

GPP as estimated with MODIS showed a pronounced decline post-fire with a pattern of GPP recovery that well-captured early- to mid-succession stages of the conceptual secondary succession model by Chapin et al. (2002). GPP was initially low and recovered faster during the first 3-4 years post-fire, with a second turning point around 9-10 years post-fire. GPP in SN-mixed conifer peaked in years 19 and 22 after fire in summer and winter, respectively, while it continued to rise in SN-ponderosa pine and KM-mixed conifer (Fig. 4d and f). We speculate that this may be followed by stable or slightly reduced GPP at the end of succession that would be associated with forest LAI reaching its maximum. Our results of post-fire GPP recovery are consistent with the dominant patterns of post-fire GPP by Goulden et al. (2011) who showed that the GPP continued to increase until year 23 after fire, after which it stabilized. In reality, a steady-state in productivity could be achieved between 20–60 years, and the required time increases with increasing latitude and correspondingly colder temperatures (Amiro et al., 2000).

Changes in ET in these sites following wildfire were observed to be consistent with changes in LAI and GPP which is unsurprising as LAI is essentially an input to the MODIS ET algorithm and a direct driver of the ET estimate. Most of the existing site-based observation studies on the impacts of wildfire on ET in Mediterranean ecosystems are limited to 5 to 15 years following fire (Dore et al., 2012; Ma et al., 2020), whereas a full recovery to pre-fire level may take longer. Here we have examined the change in ET, not only immediately following wildfire, but through 25 years post-fire. Our results showed a decrease in ET immediately after fire and gradual increase beginning with year 2 since fire. Decline in ET following wildfire have been documented in many studies (Amiro et al., 2006; Bond-Lamberty et al., 2009; Nolan et al., 2014; Roche et al., 2018) with consistent trends regardless of whether they occur in wet or dry years (Maina and Siirila-Woodburn, 2019). In this study, the mixed conifer in both ecoregions showed complete recovery to pre-fire ET levels within the 25 years post-fire (ET Anomaly $>= 0$) (Fig. 5e, g). Our results of post-fire recovery for mixed conifer are in line with the post-fire recovery of Roche et al. (2018) and Ma et al. (2020), who documented a post-fire ET recovery of ~90% (20 years post-fire) and ~80% (15 years post-fire), respectively for areas that burned with high severity with dominant vegetation comprising mixed conifers. Comparing with neighboring deciduous forest (mainly oak species) (Cocking et al., 2014; Nemens et al., 2018), our results of absolute ET reduction were higher. This may be due to other studies having lower mortality and rapid recovery by resprouting, common for oak species as present in those other study areas. Our results showed that the SN-ponderosa pine only recovered ~75% of pre-fire levels in year 25 after fire, consistent with less leaf area and higher albedo, both of which have been shown to reduce net radiation at post-burn sites (Dore et al., 2012). Lower ET after fire in ponderosa pine contrasted with other studies that documented an increase in ET after fire (Chamber and Chapin, 2002; Santos et al., 2003). One potential explanation that could explain the differences in findings between this and prior studies includes our study being conducted on semiarid region with a low LAI and limited post-fire understory grass and herbaceous expansion, unlike prior studies. In this study, we focused on a 25-year post-fire window, whereas a full recovery to stable ET conditions may require longer, particularly in case of ponderosa pine. The recovery may vary with post-fire climate, vegetation type, and ecological processes (Meng et al., 2015). Additionally, changes in biomass, density, tree size, and species composition may impact post-fire ET (Roche et al., 2018; Saksa et al., 2020); removing versus leaving woody debris on the ground can change the evaporative demand by altering land surface albedo and wetness (Walker et al., 2006; Knapp et al., 2017). The largest ET and GPP recovery occurred in regions where wildfire burned dense forest i.e., mixed conifers (Seidl et al., 2016, 2017) as these forest types that lie in wetter areas with sufficient water availability to support high primary productivity (Goulden and Bales, 2014).

We observed an increase in land surface temperature immediately after fire in both regions due to the loss of leaf area. Although the post-fire increase in albedo leads to a decrease in amount of net shortwave radiation that can contribute to surface cooling, the loss of leaf area greatly reduces the partitioning of net radiation into latent heat and associated cooling leading to heating of land surface (Chambers and Chapin, 2002). Post-fire increases in surface temperature have been documented well for several biomes in past studies (Bremer and Ham, 1999; Chambers and Chapin, 2002; Veraverbeke et al., 2012b; Liu et al., 2018, 2019). The magnitude of post-fire LST increase depends on location. Our results of post-fire LST showed an increase of LST by 11 $\pm$ 0.03 °C and 7 $\pm$ 0.01 °C in year 1 after fire in SN-mixed conifer and KM-mixed conifer, respectively (Fig. 6c). This is very similar to, if not greater than, the 5–12 °C immediate post-fire surface temperature increase reported by other studies (Amiro et al., 1999; Wendt et al., 2007; Montes-Helu et al., 2009; Veraverbeke et al., 2012b). During the subsequent post-fire summer seasons, mean LST declined sharply. This attenuation can be attributed to the recovery of LAI and char removal. Since the change in post-fire albedo is not substantial between SN-mixed conifer and KM-mixed conifer, the increase in mean LST after fire over SN-mixed conifer indicates reduction in leaf area and associated

evaporative cooling, although lower soil moisture level in Sierra Nevada region due to less precipitation would also be a contributing factor.

Finally, we must recognize errors intrinsic to land surface variables based on moderate resolution remote sensing. Although several validation comparison works have evaluated MODIS land surface products and reported that those products provide reasonable estimations of LAI, albedo, ET, GPP, and LST, these studies also showed differences between MODIS and ground-based observations due to inaccuracies in input datasets or from the coarseness of the spatial scale and interpolated meteorological inputs, increasing the uncertainty of our conclusions (Cohen et al., 2003; Heinsch et al., 2006; Coll et al., 2009; Jensen et al., 2011; Wan, 2014; Hu et al., 2015). It is important to note that MODIS biogeophysical and biogeochemical variables are inferred from the measure of surface reflectances rather than directly observed, and as a result, LAI, ET, and GPP covary. Additionally, the MODIS product algorithm relies on biome-specific values, which following extensive fire-caused mortality, can introduce additional uncertainty. For instance, MODIS products like ET and GPP are based on fPAR/LAI and the inaccurate estimation of fPAR would necessarily lead to inaccurate estimation of ET and GPP. Since land cover map is one of the variables used in MODIS fPAR algorithm, the consistently high fPAR values after fire could arise from the use of biome specific parameters. As the primary MODIS fPAR algorithm uses look-up-table (LUT) for different biomes, this could easily be a source of error in fPAR derivation if the wrong biome classification is used. Also, the MODIS GPP algorithm uses a set of biome-specific radiation use efficiency parameters ($\mathscr{E}$) that are extracted from a biome properties look-up table (BPLUT) to convert fPAR into GPP. Inaccuracies in biome classification, or within-biome variation in surface attributes, could lead to the inaccurate biome-specific radiation use efficiency parameter and ultimately poor GPP estimates. Such errors could bias our results high or low in absolute, but by calculating the change in land surface properties as an anomaly (relative to pre-fire), we obtain greater confidence in the directionality of changes over the observed time intervals. We used recovery of MODIS LAI as an indicator of vegetation recovery. LAI is a useful but imperfect indicator of vegetation change caused by wildfires. It captures some of the aggregate effects of mortality and regrowth but does not fully characterize ecosystem structural dynamics. Therefore, detailed, intensive field monitoring of vegetation structure before and after fires can be a useful complement (Williams et al., 2014), as can additional remote observations such as from lidar and radar. Moreover, relating field-level data and satellite observation can enhance the interpretability of satellite observations (Hudak et al., 2007), as well as provide a means to scale up ground observations to characterize full landscapes. Nonetheless, the strong correlation between LAI and other biophysical variables (Figs. 7 and 8) suggests that it could be applied as a useful integrative measure and predictor of post-fire ecosystem physiology and function. Our approach and results have the potential to advance the land and Earth system models, for example by using patterns emerged from our data analysis to inform model parameters that describe wildfire impacts on vegetation, hydrobiogeochemical fluxes, and land-atmosphere interactions. Our study suggests that the parameter values related to equations that describe biophysical, hydrological, and biogeochemical processes such as LAI and albedo vary over space and environmental condition, even within a vegetation type. Therefore, subtle changes to response functions relating rates of carbon, energy, and water fluxes to disturbance events and parameterization can yield divergent modeled responses of ecosystems to disturbance events. These models currently lack robust representations of the ecological and biophysical legacies from wildfire events (Lawrence and Chase, 2007; Williams et al., 2009).

5. Conclusions

This study presents a detailed account of the 25-year temporal patterns of carbon, water, and energy fluxes following wildfire in ponderosa pine and mixed conifers of Sierra Nevada and Klamath regions of the western US, a region significantly affected by wildfires in recent decades. Our analysis revealed that complete post-fire recovery of LAI in these forest ecosystems takes longer than 25 years. Post-fire changes in albedo, ET, GPP, and LST depended on changes in post-fire LAI. Summer albedo changes were minimal and declined immediately after fire; however, summer albedo increased during the subsequent summer period, whereas during winter, albedo changed by more than two-fold over the same period. We found that both ET and GPP declined sharply below pre-fire levels immediately after fire in both regions and were highly dependent on seasonality. Mixed conifers in both regions exhibited the largest ET and GPP recovery following wildfire. LST was higher after fire where it rose by 11 ± 0.03 °C and 7 ± 0.01 °C in year 1 after fire in SN-mixed conifer and KM-mixed conifer, respectively. The temperature increase became smaller as time elapsed as a consequence of vegetative regrowth. Although albedo is the main biophysical process regulating climate at high latitudes (Bonan, 2008), this study showed that strong decreases in ET and associated decreases in summer cooling outweigh the changes in post-fire albedo as the main factor controlling the immediate post-fire annual warming effect of wildfires in the mountainous regions of the western US. Our results can be used to predict ecological responses to wildfire in these and similar ecoregions as they represent mean historical behavior across several disturbance events. By aggregating across many fire events and arraying observations along a 25-year chronosequence, these results provide a useful guide for assessing local fluxes of carbon, water, and energy associated with wildfire disturbance and forest recovery, and for advancing models to incorporate post-fire dynamics. Furthermore, future research on biogeophysical and biogeochemical impacts of wildfire guided by field-based observations, research that separates over- and understory impacts in particular, will increase the confidence of our findings.

Declaration of Competing Interest

The authors declare that they have no known competing financial interests or personal relationships that could have appeared to influence the work reported in this paper.

The authors declare the following financial interests/personal relationships which may be considered as potential competing interests.

References

Abatzoglou, J.T., Williams, A.P., 2016. Impact of anthropogenic climate change on wildfire across western US forests. Proc. Natl. Acad. Sci. 113, 11770–11775. https://doi.org/10.1073/pnas.1607171113.

Amiro, B.D., MacPherson, J.I., Desjardins, R.L., 1999. BOREAS flight measurements of forest-fire effects on carbon dioxide and energy fluxes. Agric. For. Meteorol. 96, 199–208. https://doi.org/10.1016/S0168-1923(99)00050-7.

Amiro, B.D., Chen, J.M., Liu, J., 2000. Net primary productivity following forest fire for Canadian ecoregions. Can. J. For. Res. 30, 939–947. https://doi.org/10.1139/cjfr-30-6-939.

Amiro, B.D., Orchansky, A.L., Barr, A.G., Black, T.A., Chambers, S.D., Chapin, F.S., Goulden, M.L., Litvak, M., Liu, H.P., McCaughey, J.H., McMillan, A., Randerson, J. T., 2006. The effect of post-fire stand age on the boreal forest energy balance. Agric. For. Meteorol. 140, 41–50. https://doi.org/10.1016/j.agrformet.2006.02.014.

Amiro, B.D., Barr, A.G., Barr, J.G., Black, T.A., Bracho, R., Brown, M., Chen, J., Clark, K. L., Davis, K.J., Desai, A.R., Dore, S., Engel, V., Fuentes, J.D., Goldstein, A.H., Goulden, M.L., Kolb, T.E., Lavigne, M.B., Law, B.E., Margolis, H.A., Martin, T., McCaughey, J.H., Misson, L., Montes-Helu, M., Noormets, A., Randerson, J.T., Starr, G., Xiao, J., 2010. Ecosystem carbon dioxide fluxes after disturbance in forests of North America. J. Geophys. Res. Biogeosci. 115 https://doi.org/10.1029/2010JG001390.

Archibald, S., Lehmann, C.E.R., Belcher, C.M., Bond, W.J., Bradstock, R.A., Daniau, A.L., Dexter, K.G., Forrestel, E.J., Greve, M., He, T., Higgins, S.I., Hoffmann, W.A., Lamont, B.B., McGlinn, D.J., Moncrieff, G.R., Osborne, C.P., Pausas, J.G., Price, O., Ripley, B.S., Rogers, B.M., Schwilk, D.W., Simon, M.F., Turetsky, M.R., V. der Werf, G.R., Zanne, A.E., 2018. Biological and geophysical feedbacks with fire in the earth system. Environ. Res. Lett. 13, 033003 https://doi.org/10.1088/1748-9326/aa9ead.

Balch, J.K., Bradley, B.A., Abatzoglou, J.T., Chelsea Nagy, R., Fusco, E.J., Mahood, A.L., 2017. Human-started wildfires expand the fire niche across the United States. Proc. Natl. Acad. Sci. USA. 114, 2946–2951. https://doi.org/10.1073/pnas.1617394114.

Beringer, J., Hutley, L.B., Tapper, N.J., Coutts, A., Kerley, A., O'Grady, A.P., 2003. Fire impacts on surface heat, moisture and carbon fluxes from a tropical savanna in

northern Australia. Int. J. Wildl. Fire 12, 333–340. https://doi.org/10.1071/wf03023.
Bhattarai, N., Mallick, K., Brunsell, N.A., Sun, G., Jain, M., 2018. Regional evapotranspiration from an image-based implementation of the surface temperature initiated closure (STIC1.2) model and its validation across an aridity gradient in the conterminous US. Hydrol. Earth Syst. Sci. 22, 2311–2341. https://doi.org/10.5194/hess-22-2311-2018.
Bonan, G.B., 2008. Forests and climate change: forcings, feedbacks, and the climate benefits of forests. Science 320 (5882), 1444–1449. https://doi.org/10.1126/science.1155121.
Bond-Lamberty, B., Peckham, S.D., Gower, S.T., Ewers, B.E., 2009. Effects of fire on regional evapotranspiration in the central Canadian boreal forest. Glob. Chang. Biol. 15, 1242–1254. https://doi.org/10.1111/j.1365-2486.2008.01776.x.
Bowman, D.M.J.S., Balch, J.K., Artaxo, P., Bond, W.J., Jean, M., Cochrane, M.A., Antonio, C.M.D., Defries, R.S., Doyle, J.C., Harrison, P., Johnston, F.H., Keeley, J.E., Krawchuk, M.A., Kull, C.A., Marston, B., Moritz, M.A., Prentice, I.C., Roos, C.I., Scott, A.C., Swetnam, T.W., Werf, G.R., Van Der, P.S.J., 2009. Fire in the earth system. Science 324. https://doi.org/10.1126/science.1163886.
Bremer, D.J., Ham, J.M., 1999. Effect of spring burning on the surface energy balance in a tallgrass prairie. Agric. For. Meteorol. 97, 43–54. https://doi.org/10.1016/S0168-1923(99)00034-9.
Bright, B.C., Hicke, J.A., Meddens, A.J.H., 2013. Effects of bark beetle-caused tree mortality on biogeochemical and biogeophysical MODIS products. J. Geophys. Res. Biogeosciences 118, 974–982. https://doi.org/10.1002/jgrg.20078.
Bright, B.C., Hudak, A.T., Kennedy, R.E., Braaten, J.D., Henareh Khalyani, A., 2019. Examining post-fire vegetation recovery with landsat time series analysis in three western North American forest types. Fire Ecol. 15 https://doi.org/10.1186/s42408-018-0021-9.
Chambers, S.D., Chapin, F.S., 2002. Fire effects on surface-atmosphere energy exchange in Alaskan black spruce ecosystems fire effects on surface-atmosphere energy exchange in Alaskan black spruce ecosystems: implications for feedbacks to regional climate. J. Geophys. Res. 107, 8145. https://doi.org/10.1029/2001JD000530.
Chambers, S.D., Beringer, J., Randerson, J.T., Chapin, I.S., 2005. Fire effects on net radiation and energy partitioning: Contrasting responses of tundra and boreal forest ecosystems. J. Geophys. Res. 110, 1–9. https://doi.org/10.1029/2004JD005299.
Chapin, F.S., Matson, P.A., Mooney, H.A., 2002. Principles of Terrestrial Ecosystem Ecology. Springer, New York, USA.
Chen, X., Vogelmann, J.E., Rollins, M., Ohlen, D., Key, C.H., Yang, L., Huang, C., Shi, H., 2011. Detecting post-fire burn severity and vegetation recovery using multitemporal remote sensing spectral indices and field-collected composite burn index data in a ponderosa pine forest. Int. J. Remote Sens. 32, 7905–7927. https://doi.org/10.1080/01431161.2010.524678.
Chu, T., Guo, X., 2014. Remote sensing techniques in monitoring post-fire effects and patterns of forest recovery in Boreal forest regions: a review. Remote Sens 6, 470–520. https://doi.org/10.3390/rs6010470.
Chuvieco, E., Englefield, P., Trishchenko, A.P., Luo, Y., 2008. Generation of long time series of burn area maps of the boreal forest from NOAA-AVHRR composite data. Remote Sens. Environ. 112, 2381–2396. https://doi.org/10.1016/j.rse.2007.11.007.
Cocking, M.I., Varner, J.M., Knapp, E.E., 2014. Long-term effects of fire severity on oak-conifer dynamics in the southern Cascades. Ecol. Appl. 24, 94–107. https://doi.org/10.1890/13-0473.1.
Cohen, W.B., Maiersperger, T.K., Yang, Z., Gower, S.T., Turner, D.P., Ritts, W.D., Berterretche, M., Running, S.W., 2003. Comparisons of land cover and LAI estimates derived from ETM+ and MODIS for four sites in North America: a quality assessment of 2000/2001 provisional MODIS products. Remote Sens. Environ. 88, 233–255. https://doi.org/10.1016/j.rse.2003.06.006.
Cohen, W.B., Maiersperger, T.K., Turner, D.P., Ritts, W.D., Pflugmacher, D., Kennedy, R. E., Kirschbaum, A., Running, S.W., Costa, M., Gower, S.T., 2006. MODIS land cover and LAI collection 4 product quality across nine sites in the western hemisphere. IEEE Trans. Geosci. Remote Sens. 44, 1843–1857. https://doi.org/10.1109/TGRS.2006.876026.
Coll, C., Wan, Z., Galve, J.M., 2009. Temperature-based and radiance-based validations of the V5 MODIS land surface temperature product. J. Geophys. Res. Atmos. 114, 1–15. https://doi.org/10.1029/2009JD012038.
Dennison, P.E., Brewer, S.C., Arnold, J.D., Moritz, M.A., 2014. Large wildfire trends in the western United States, 1984–2011. Geophys. Res. Lett. 41, 2928–2933. https://doi.org/10.1002/2014GL059576.
Domingo, F., Villagarcía, L., Brenner, A.J., Puigdefábregas, J., 2000. Measuring and modelling the radiation balance of a heterogeneous Shrubland. Plant Cell Environ. 23, 27–38. https://doi.org/10.1046/j.1365-3040.2000.00532.x.
Dore, A.S., Kolb, T.E., Eckert, S.E., Sullivan, B.W., Hungate, B.A., Kaye, J.P., Hart, S.C., Koch, G.W., Finkral, A., Applications, S.E., April, N., Dore, S., Kolb, T.E., Eckert, S.E., Sullivan, W., Hungate, B.A., Kaye, J.P., 2010. Carbon and water fluxes from ponderosa pine forests disturbed by wildfire and thinning. Ecol. Appl. 20, 663–683.
Dore, S., Montes-Helu, M., Hart, S.C., Hungate, B.A., Koch, G.W., Moon, J.B., Finkral, A. J., Kolb, T.E., 2012. Recovery of ponderosa pine ecosystem carbon and water fluxes from thinning and stand-replacing fire. Glob. Chang. Biol. 18, 3171–3185. https://doi.org/10.1111/j.1365-2486.2012.02775.x.
Eidenshink, J., Schwind, B., Brewer, K., Zhu, Z., Quayle, B., Howard, S., Falls, S., Falls, S., 2007. A project for monitoring trends in burn severity. Fire Ecol. Spec. Issue 3, 3–21.
Epting, J., Verbyla, D., 2005. Landscape-level interactions of prefire vegetation, burn severity, and postfire vegetation over a 16-year period in interior Alaska. Can. J. For. Res. 35, 1367–1377. https://doi.org/10.1139/x05-060.
Feng, X.M., Sun, G., Fu, B.J., Su, C.H., Liu, Y., Lamparski, H., 2012. Regional effects of vegetation restoration on water yield across the Loess Plateau, China. Hydrol. Earth Syst. Sci. 16, 2617–2628. https://doi.org/10.5194/hess-16-2617-2012.
French, N.H.F., Kasischke, E.S., Hall, R.J., Murphy, K.A., Verbyla, D.L., Hoy, E.E., Allen, J.L., 2008. Using Landsat data to assess fire and burn severity in the North American boreal forest region: an overview and summary of results. Int. J. Wildl. Fire 17, 443–462.
Gao, F., Schaaf, C.B., Strahler, A.H., Roesch, A., Lucht, W., Dickinson, R., 2005. MODIS bidirectional reflectance distribution function and albedo climate modeling grid products and the variability of albedo major global vegetation types. J. Geophys. Res. D Atmos. 110, 1–13. https://doi.org/10.1029/2004JD005190.
Ghimire, B., Williams, C.A., Collatz, G.J., Vanderhoof, M., 2012. Fire-induced carbon emissions and regrowth uptake in western U. S. forests: documenting variation across forest types, fire severity, and climate regions. J. Geophys. Res. 117, 1–29. https://doi.org/10.1029/2011JG001935.
Giglio, L., Randerson, J.T., Van Der Werf, G.R., Kasibhatla, P.S., Collatz, G.J., Morton, D. C., Defries, R.S., 2010. Assessing variability and long-term trends in burned area by merging multiple satellite fire products. Biogeosciences 7, 1171–1186. https://doi.org/10.5194/bg-7-1171-2010.
Giglio, L., Boschetti, L., Roy, D.P., Humber, M.L., Justice, C.O., 2018. The collection 6 MODIS burned area mapping algorithm and product. Remote Sens. Environ. 217, 72–85. https://doi.org/10.1016/j.rse.2018.08.005.
Gleason, K.E., McConnell, J.R., Arienzo, M.M., Chellman, N., Calvin, W.M., 2019. Four-fold increase in solar forcing on snow in western U.S. burned forests since 1999. Nat. Commun. 10, 1–8. https://doi.org/10.1038/s41467-019-09935-y.
Goulden, M.L., Bales, R.C., 2014. Mountain runoff vulnerability to increased evapotranspiration with vegetation expansion. Proc. Natl. Acad. Sci. USA. 111, 14071–14075. https://doi.org/10.1073/pnas.1319316111.
Goulden, M.L., Mcmillan, A.M.S., Winston, G.C., Rocha, A.V., Manies, K.L., Harden, J.W., Bond-Lamberty, B.P., 2011. Patterns of NPP, GPP, respiration, and NEP during boreal forest succession. Glob. Chang. Biol. 17, 855–871. https://doi.org/10.1111/j.1365-2486.2010.02274.x.
Grabinski, Z.S., Sherriff, R.L., Kane, J.M., 2017. Controls of reburn severity vary with fire interval in the Klamath Mountains, California, USA. Ecosphere 8. https://doi.org/10.1002/ecs2.2012.
Guz, J., Gill, N.S., Kulakowski, D., 2021. Long-term empirical evidence shows post-disturbance climate controls post-fire regeneration. J. Ecol. https://doi.org/10.1111/1365-2745.13771.
Heinsch, F.A., Zhao, M., Running, S.W., Kimball, J.S., Nemani, R.R., Davis, K.J., Bolstad, P.V., Cook, B.D., Desai, A.R., Ricciuto, D.M., Law, B.E., Oechel, W.C., Kwon, H., Luo, H., Wofsy, S.C., Dunn, A.L., Munger, J.W., Baldocchi, D.D., Xu, L., Hollinger, D.Y., Richardson, A.D., Stoy, P.C., Siqueira, M.B.S., Monson, R.K., Burns, S.P., Flanagan, L.B., 2006. Evaluation of remote sensing based terrestrial productivity from MODIS using regional tower eddy flux network observations. IEEE Trans. Geosci. Remote Sens. 44, 1908–1923. https://doi.org/10.1109/TGRS.2005.853936.
Hessburg, P.F., Prichard, S.J., Hagmann, R.K., Povak, N.A., Lake, F.K., 2021. Wildfire and climate change adaptation of western North American forests: a case for intentional management. Ecol. Appl. 31 (8). https://doi.org/10.1002/eap.2432.
Hope, A., Tague, C., Clark, R., 2007. Characterizing post-fire vegetation recovery of California chaparral using TM/ETM+ time-series data. Int. J. Remote Sens. 28, 1339–1354. https://doi.org/10.1080/01431160600908924.
Hu, G., Jia, L., Menenti, M., 2015. Comparison of MOD16 and LSA-SAF MSG evapotranspiration products over Europe for 2011. Remote Sens. Environ. 156, 510–526. https://doi.org/10.1016/j.rse.2014.10.017.
Hudak, A.T., Morgan, P., Bobbitt, M.J., Smith, A.M.S., Lewis, S.A., Lentile, L.B., Robichaud, P.R., Clark, J.T., McKinley, R.A., 2007. The relationship of multispectral satellite imagery to immediate fire effects. Fire Ecol. 3, 64–90. https://doi.org/10.4996/fireecology.0301064.
Huete, A., Didan, K., Miura, T., Rodriguez, E.P., Gao, X., Ferreira, L.G., 2002. Overview of the radiometric and biophysical performance of the MODIS vegetation indices. Remote Sens. Environ. 83 (1–2), 195–213. https://doi.org/10.1016/S0034-4257(02)00096-2.
Jensen, J.L.R., Humes, K.S., Hudak, A.T., Vierling, L.A., Delmelle, E., 2011. Evaluation of the MODIS LAI product using independent lidar-derived LAI: A case study in mixed conifer forest. Remote Sens. Environ. 115, 3625–3639. https://doi.org/10.1016/j.rse.2011.08.023.
Jin, Y., Roy, D.P., 2005. Fire-induced albedo change and its radiative forcing at the surface in Northern Australia. Geophys. Res. Lett. 32, 1–4. https://doi.org/10.1029/2005GL022822.
Jin, Y., Randerson, J.T., Goetz, S.J., Beck, P.S.A., Loranty, M.M., Goulden, M.L., 2012. The influence of burn severity on postfire vegetation recovery and albedo change during early succession in North American boreal forests. J. Geophys. Res. Biogeosci. 117, 1–15. https://doi.org/10.1029/2011JG001886.
Keeley, J.E., 2009. Fire intensity, fire severity and burn severity: a brief review and suggested usage. Int. J. Wildl. Fire 18, 116–126. https://doi.org/10.1071/WF07049.
Kim, H.W., Hwang, K., Mu, Q., Lee, S.O., Choi, M., 2012. Validation of MODIS 16 global terrestrial evapotranspiration products in various climates and land cover types in Asia. KSCE J. Civ. Eng. 16, 229–238. https://doi.org/10.1007/s12205-012-0006-1.
Knapp, E.E., Lydersen, J.M., North, M.P., Collins, B.M., 2017. Efficacy of variable density thinning and prescribed fire for restoring forest heterogeneity to mixed-conifer forest in the central Sierra Nevada, CA. For. Ecol. Manag. 406, 228–241. https://doi.org/10.1016/j.foreco.2017.08.028.
Lanorte, A., Danese, M., Lasaponara, R., Murgante, B., 2013. Multiscale mapping of burn area and severity using multisensor satellite data and spatial autocorrelation analysis. Int. J. Appl. Earth Obs. Geoinf. 20, 42–51. https://doi.org/10.1016/j.jag.2011.09.005.

Lawrence, P.J., Chase, T.N., 2007. Representing a new MODIS consistent land surface in the community land model (CLM 3.0). J. Geophys. Res. Biogeosci. 112 https://doi.org/10.1029/2006JG000168.
Lentile, L.B., Holden, Z.A., Smith, A.M.S., Falkowski, M.J., Hudak, A.T., Morgan, P., Lewis, S.A., Gessler, P.E., Benson, N.C., 2006. Remote sensing techniques to assess active fire characteristics and post-fire effects. Int. J. Wildl. Fire 15, 319–345.
Li, F., Lawrence, D.M., Bond-Lamberty, B., 2017. Impact of fire on global land surface air temperature and energy budget for the 20th century due to changes within ecosystems. Environ. Res. Lett. 12 https://doi.org/10.1088/1748-9326/aa6685.
Littell, J.S., Mckenzie, D., Peterson, D.L., Westerling, A.L., 2009. Climate and wildfire area burned in western U.S. ecoprovinces, 191 6-2003. Ecol. Appl. 19, 1003–1021.
Liu, H., Randerson, J.T., Lindfors, J., Iii, F.S.C., 2005. Changes in the surface energy budget after fire in boreal ecosystems of interior Alaska: an annual perspective. J. Geophys. Res. Atmos. 110, 1–12. https://doi.org/10.1029/2004JD005158.
Liu, Z., Ballantyne, A.P., Cooper, L.A., 2018. Increases in land surface temperature in response to fire in siberian boreal forests and their attribution to biophysical processes. Geophys. Res. Lett. 45, 6485–6494. https://doi.org/10.1029/2018GL078283.
Liu, Z., Ballantyne, A.P., Cooper, L.A., 2019. Biophysical feedback of global forest fires on surface temperature. Nat. Commun. 10, 1–9. https://doi.org/10.1038/s41467-018-08237-z.
Loboda, T.V., Hoy, E.E., Giglio, L., Kasischke, E.S., 2011. Mapping burned area in Alaska using MODIS data: a data limitations-driven modification to the regional burned area algorithm. Int. J. Wildl. Fire 20, 487–496. https://doi.org/10.1071/WF10017.
Lutz, J.A., van Wagtendonk, J.W., Franklin, J.F., 2009. Twentieth-century decline of large-diameter trees in Yosemite National Park, California, USA. For. Ecol. Manag. 257, 2296–2307. https://doi.org/10.1016/j.foreco.2009.03.009.
Lyons, E.A., Jin, Y., Randerson, J.T., 2008. Changes in surface albedo after fire in boreal forest ecosystems of interior Alaska assessed using MODIS satellite observations. J. Geophys. Res. Biogeosci. 113, 1–15. https://doi.org/10.1029/2007JG000606.
Ma, Q., Bales, R.C., Rungee, J., Conklin, M.H., Collins, B.M., Goulden, M.L., 2020. Wildfire controls on evapotranspiration in California's Sierra Nevada. J. Hydrol. 590, 125364 https://doi.org/10.1016/j.jhydrol.2020.125364.
Maina, F.Z., Siirila-Woodburn, E.R., 2019. Watersheds dynamics following wildfires: nonlinear feedbacks and implications on hydrologic responses. Hydrol. Process. 34, 33–50. https://doi.org/10.1002/hyp.13568.
Martel, M.C., Margolis, H.A., Coursolle, C., Bigras, F.J., Heinsch, F.A., Running, S.W., 2005. Decreasing photosynthesis at different spatial scales during the late growing season on a boreal cutover. Tree Physiol. 25, 689–699. https://doi.org/10.1093/treephys/25.6.689.
Masek, J.G., Goward, S.N., Kennedy, R.E., Warren, B., Moisen, G.G., Schleeweis, K., Huang, C., 2013. United States Forest Disturbance Trends Observed Using Landsat Time Series. Ecosystems 16, 1087–1104. https://doi.org/10.1007/s10021-013-9669-9.
McLauchlan, K.K., Higuera, P.E., Miesel, J., Rogers, B.M., Schweitzer, J., Shuman, J.K., Tepley, A.J., Varner, J.M., Veblen, T.T., Adalsteinsson, S.A., Balch, J.K., Baker, P., Batllori, E., Bigio, E., Brando, P., Cattau, M., Chipman, M.L., Coen, J., Crandall, R., Daniels, L., Enright, N., Gross, W.S., Harvey, B.J., Hatten, J.A., Hermann, S., Hewitt, R.E., Kobziar, L.N., Landesmann, J.B., Loranty, M.M., Maezumi, S.Y., Mearns, L., Moritz, M., Myers, J.A., Pausas, J.G., Pellegrini, A.F.A., Platt, W.J., Roozeboom, J., Safford, H., Santos, F., Scheller, R.M., Sherriff, R.L., Smith, K.G., Smith, M.D., Watts, A.C., 2020. Fire as a fundamental ecological process: research advances and frontiers. J. Ecol. 108, 2047–2069. https://doi.org/10.1111/1365-2745.13403.
Meng, R., Dennison, P.E., D'Antonio, C.M., Moritz, M.A., 2014. Remote sensing analysis of vegetation recovery following short-interval fires in Southern California Shrublands. PLoS One 9, 14–17. https://doi.org/10.1371/journal.pone.0110637.
Meng, R., Dennison, P.E., Huang, C., Moritz, M.A., D'Antonio, C., 2015. Effects of fire severity and post-fire climate on short-term vegetation recovery of mixed-conifer and red fir forests in the Sierra Nevada Mountains of California. Remote Sens. Environ. 171, 311–325. https://doi.org/10.1016/j.rse.2015.10.024.
Micheletty, P.D., Kinoshita, A.M., Hogue, T.S., 2014. Application of MODIS snow cover products: wildfire impacts on snow and melt in the Sierra Nevada. Hydrol. Earth Syst. Sci. 18, 4601–4615. https://doi.org/10.5194/hess-18-4601-2014.
Miller, J.D., Thode, A.E., 2007. Quantifying burn severity in a heterogeneous landscape with a relative version of the delta normalized burn ratio (dNBR). Remote Sens. Environ. 109, 66–80. https://doi.org/10.1016/j.rse.2006.12.006.
Montes-Helu, M.C., Kolb, T., Dore, S., Sullivan, B., Hart, S.C., Koch, G., Hungate, B.A., 2009. Persistent effects of fire-induced vegetation change on energy partitioning and evapotranspiration in ponderosa pine forests. Agric. For. Meteorol. 149, 491–500. https://doi.org/10.1016/j.agrformet.2008.09.011.
Morgan, P., Heyerdahl, E.K., Gibson, C.E., 2008. Multi-season climate synchronized forest fires throughout the 20th century, Northern Rockies, USA. Ecology 89, 717–728. https://doi.org/10.1890/06-2049.1.
Mu, Q., Zhao, M., Running, S.W., 2011. Improvements to a MODIS global terrestrial evapotranspiration algorithm. Remote Sens. Environ. 115, 1781–1800. https://doi.org/10.1016/j.rse.2011.02.019.
Myneni, R.B., Hoffman, S., Knyazikhin, Y., Privette, J.L., Glassy, J., Tian, Y., Wang, Y., Song, X., Zhang, Y., Smith, G.R., Lotsch, A., Friedl, M., Morisette, J.T., Votava, P., Nemani, R.R., Running, S.W., 2002. Global products of vegetation leaf area and fraction absorbed PAR from year one of MODIS data. Remote Sens. Environ. 83, 214–231. https://doi.org/10.1016/S0034-4257(02)00074-3.
NIFC [National Interagency Fire Center], 2020. National Report of Wildland Fires and Acres Burned by State. https://www.nifc.gov/fireInfo/fireInfo_statistics.html. Accessed 15 February 2020.
Nemani, R.R., Keeling, C.D., Hashimoto, H., Jolly, W.M., Piper, S.C., Tucker, C.J., Myneni, R.B., Running, S.W., 2003. Climate-driven increases in global terrestrial net primary production from 1982 to 1999. Science 300, 1560–1563. https://doi.org/10.1126/science.1082750.
Nemens, D.G., Varner, J.M., Kidd, K.R., Wing, B., 2018. Do repeated wildfires promote restoration of oak woodlands in mixed-conifer landscapes? For. Ecol. Manag. 427, 143–151. https://doi.org/10.1016/j.foreco.2018.05.023.
Nolan, R.H., Lane, P.N.J., Benyon, R.G., Bradstock, R.A., Mitchell, P.J., 2014. Changes in evapotranspiration following wildfire in resprouting eucalypt forests. Ecohydrology 7, 1363–1377. https://doi.org/10.1002/eco.1463.
North, M., 2012. Managing Sierra Nevada forests. US Department of Agriculture, Forest Service, Pacific Southwest Research Station, Albany, CA, p. 184 p. Gen Tech Rep PSW-GTR-237.
O'Halloran, T.L., Law, B.E., Goulden, M.L., Wang, Z., Barr, J.G., Schaaf, C., Brown, M., Fuentes, J.D., Göckede, M., Black, A., Engel, V., 2012. Radiative forcing of natural forest disturbances. Glob. Chang. Biol. 18, 555–565. https://doi.org/10.1111/j.1365-2486.2011.02577.x.
O'Halloran, T.L., Acker, S.A., Joerger, V.M., Kertis, J., Law, B.E., 2014. Postfire influences of snag attrition on albedo and radiative forcing. Geophys. Res. Lett. 41, 9135–9142. https://doi.org/10.1002/2014GL062024.Received.
Parks, S.A., Abatzoglou, J.T., 2020. Warmer and drier fire seasons contribute to increases in area burned at high severity in Western US forests from 1985 to 2017. Geophys. Res. Lett. 47, 0–2. https://doi.org/10.1029/2020GL089858.
Randerson, J.T., Liu, H., Flanner, M.G., Chambers, S.D., Jin, Y., Hess, P.G., Pfister, G., Mack, M.C., Treseder, K.K., Welp, L.R., Chapin, F.S., Harden, J.W., Goulden, M.L., Neff, J.C., Schuur, E.A.G., Zender, C.S., 2006. The impact of boreal forest fire on climate warming. Science 314, 1130. https://doi.org/10.1126/science.1132075.
Roche, J.W., Goulden, M.L., Bales, R.C., 2018. Estimating evapotranspiration change due to forest treatment and fire at the basin scale in the Sierra Nevada, California. Ecohydrology 11. https://doi.org/10.1002/eco.1978.
Roche, J.W., Ma, Q., Rungee, J., Bales, R.C., 2020. Evapotranspiration mapping for forest management in California's Sierra Nevada. Front. For. Glob. Chang. 3, 1–14. https://doi.org/10.3389/ffgc.2020.00069.
Rogan, J., Franklin, J., 2001. Mapping wildfire burn severity in Southern California forests and shrublands using enhanced thematic mapper imagery. Geocarto Int. 16, 91–106. https://doi.org/10.1080/10106040108542218.
Rogers, B.M., Neilson, R.P., Drapek, R., Lenihan, J.M., Wells, J.R., Bachelet, D., Law, B.E., 2011. Impacts of climate change on fire regimes and carbon stocks of the U.S. Pacific Northwest. J. Geophys. Res. Biogeosci. 116, 1–13. https://doi.org/10.1029/2011JG001695.
Rogers, B.M., Randerson, J.T., Bonan, G.B., 2013. High-latitude cooling associated with landscape changes from North American boreal forest fires. Biogeosciences 10, 699–718. https://doi.org/10.5194/bg-10-699-2013.
Rogers, B.M., Soja, A.J., Goulden, M.L., Randerson, J.T., 2015. Influence of tree species on continental differences in boreal fires and climate feedbacks. Nat. Geosci. 8, 228–234. https://doi.org/10.1038/ngeo2352.
Ruefenacht, B., Finco, M., Czaplewski, R., Helmer, E., Blackard, J., Holden, G., Lister, A., Salajanu, D., Weyermann, D., Winterberger, K., 2008. Conterminous US and Alaska forest type mapping using forest inventory and analysis data. Photogramm. Eng. Remote Sens. 74, 1379–1388.
Running, S.W., Nemani, R.R., Heinsch, F.A., Zhao, M., Reeves, M., Hashimoto, H., 2004. A continuous satellite-derived measure of global terrestrial primary production. Bioscience 54, 547–560. https://doi.org/10.1641/0006-3568(2004)054[0547:ACSMOG]2.0.CO;2.
Saksa, P.C., Bales, R.C., Tague, C.L., Battles, J.J., Tobin, B.W., Conklin, M.H., 2020. Fuels treatment and wildfire effects on runoff from Sierra Nevada mixed-conifer forests. Ecohydrology 13. https://doi.org/10.1002/eco.2151.
Salomonson, V.V., Appel, I., 2004. Estimating fractional snow cover from MODIS using the normalized difference snow index. Remote Sensing of Environment 89 (3), 351–360. https://doi.org/10.1016/j.rse.2003.10.016.
Santos, A.J.B., Silva, G.T.D.A., Miranda, H.S., Miranda, A.C., Lloyd, J., 2003. Effects of fire on surface carbon, energy and water vapour fluxes over campo sujo savanna in central Brazil. Funct. Ecol. 17, 711–719. https://doi.org/10.1111/j.1365-2435.2003.00790.x.
Schaaf, C.B., Gao, F., Strahler, A.H., Lucht, W., Li, X., Tsang, T., Strugnell, N.C., Zhang, X., Jin, Y., Muller, J., Lewis, P., Barnsley, M., Hobson, P., Disney, M., Roberts, G., Dunderdale, M., Doll, C., Robert, P., Hu, B., Liang, S., Privette, J.L., Roy, D., 2002. First operational BRDF, albedo nadir reflectance products from MODIS. Remote Sens. Environ. 83, 135–148.
Seidl, R., Spies, T.A., Peterson, D.L., Stephens, S.L., Hicke, J.A., 2016. Searching for resilience: addressing the impacts of changing disturbance regimes on forest ecosystem services. J. Appl. Ecol. 53, 120–129. https://doi.org/10.1111/1365-2664.12511.
Seidl, R., Thom, D., Kautz, M., Martin-Benito, D., Peltoniemi, M., Vacchiano, G., Wild, J., Ascoli, D., Petr, M., Honkaniemi, J., Lexer, M.J., Trotsiuk, V., Mairota, P., Svoboda, M., Fabrika, M., Nagel, T.A., Reyer, C.P.O., 2017. Forest disturbances under climate change. Nat. Clim. Chang. 7, 395–402. https://doi.org/10.1038/nclimate3303.
Stephens, S.L., Moghaddas, J.J., Edminster, C., Fiedler, C.E., Haase, S., Harrington, M., Keeley, J.E., Knapp, E.E., Mciver, J.D., Metlen, K., Skinner, C.N., Youngblood, A., 2009. Fire treatment effects on vegetation structure, fuels, and potential fire severity in western U.S. forests. Ecol. Appl. 19, 305–320. https://doi.org/10.1890/07-1755.1.
Stevens-Rumann, C.S., Morgan, P., 2019. Tree regeneration following wildfires in the western US: a review. Fire Ecol. 15, 1–17.

Stoddard, M.T., Huffman, D.W., Fulé, P.Z., Crouse, J.E., Meador, A.J.S., 2018. Forest structure and regeneration responses 15 years after wildfire in a ponderosa pine and mixed-conifer ecotone, Arizona, USA. Fire Ecol. 14, 1–12. https://doi.org/10.1186/s42408-018-0011-y.

Storey, E.A., Stow, D.A., Leary, J.F.O., 2016. Assessing post fire recovery of chamise chaparral using multi-temporal spectral vegetation index trajectories derived from Landsat imagery. Remote Sens. Environ. 183, 53–64. https://doi.org/10.1016/j.rse.2016.05.018.

Tepley, A.J., Thompson, J.R., Epstein, H.E., Anderson-Teixeira, K.J., 2017. Vulnerability to forest loss through altered post fire recovery dynamics in a warming climate in the Klamath Mountains. Glob. Chang. Biol. 23, 4117–4132. https://doi.org/10.1111/gcb.13704.

Thompson, C., Beringer, J., Chapin, F.S., McGuire, A.D., 2004. Structural complexity and land-surface energy exchange along a gradient from arctic tundra to boreal forest. J. Veg. Sci. 15, 397–406. https://doi.org/10.1111/j.1654-1103.2004.tb02277.x.

Thornton, P.E., Law, B.E., Gholz, H.L., Clark, K.L., Falge, E., Ellsworth, D.S., Goldstein, A. H., Monson, R.K., Hollinger, D., Falk, M., Chen, J., Sparks, J.P., 2002. Modeling and measuring the effects of disturbance history and climate on carbon and water budgets in evergreen needleleaf forests. Agric. For. Meteorol. 113, 185–222.

Vanderhoof, M., Williams, C.A., Shuai, Y., Jarvis, D., Kulakowski, D., Masek, J., Technology, R., 2014. Albedo-induced radiative forcing from mountain pine beetle outbreaks in forests, south-central rocky mountains: magnitude, persistence, and relation to outbreak severity. Biogeosciences 11, 563–575. https://doi.org/10.5194/bg-11-563-2014.

Veraverbeke, S., Lhermitte, S., Verstraeten, W.W., Goossens, R., 2010. The temporal dimension of differenced normalized burn ratio (dNBR) fire/burn severity studies: the case of the large 2007 Peloponnese wildfires in Greece. Remote Sens. Environ. 114, 2548–2563. https://doi.org/10.1016/j.rse.2010.05.029.

Veraverbeke, S., Gitas, I., Katagis, T., Polychronaki, A., Somers, B., Goossens, R., 2012a. Assessing post-fire vegetation recovery using red-near infrared vegetation indices: Accounting for background and vegetation variability. ISPRS J. Photogramm. Remote Sens. 68, 28–39. https://doi.org/10.1016/j.isprsjprs.2011.12.007.

Veraverbeke, S., Verstraeten, W.W., Lhermitte, S., Van De Kerchove, R., Goossens, R., 2012b. Assessment of post-fire changes in land surface temperature and surface albedo, and their relation with fireburn severity using multitemporal MODIS imagery. Int. J. Wildl. Fire 21, 243–256. https://doi.org/10.1071/WF10075.

Viedma, O., Meliá, J., Segarra, D., García-Haro, J., 1997. Modeling rates of ecosystem recovery after fires by using Landsat TM data. Remote Sens. Environ. 61, 383–398. https://doi.org/10.1016/S0034-4257(97)00048-5.

Walker, R.F., Johnson, D.W., Miller, W.W., Fecko, R.M., Murphy, J.D., Frederick, W.B., 2006. Thinning and prescribed fire effects on forest floor fuels in the east side Sierra Nevada pine type. J. Sustain. For. 23, 99–115. https://doi.org/10.1300/J091v23n02_06.

Wan, Z., 2008. New refinements and validation of the MODIS Land-Surface Temperature/Emissivity products. Remote Sens. Environ. 112, 59–74. https://doi.org/10.1016/j.rse.2006.06.026.

Wan, Z., 2014. New refinements and validation of the collection-6 MODIS land-surface temperature/emissivity product. Remote Sens. Environ. 140, 36–45. https://doi.org/10.1016/j.rse.2013.08.027.

Ward, D.S., Kloster, S., Mahowald, N.M., Rogers, B.M., Randerson, J.T., Hess, P.G., 2012. The changing radiative forcing of fires: global model estimates for past, present and future. Atmos. Chem. Phys. 12, 10857–10886. https://doi.org/10.5194/acp-12-10857-2012.

Wendt, C.K., Beringer, J., Tapper, N.J., Hutley, L.B., 2007. Local boundary-layer development over burnt and unburnt tropical savanna: an observational study. Boundary-Layer Meteorol. 124, 291–304. https://doi.org/10.1007/s10546-006-9148-3.

Westerling, A.L., Hidalgo, H.G., Cayan, D.R., Swetnam, T.W., 2006. Warming and earlier spring increase western U. S. forest wildfire activity. Science. 313, 940–943.

Westerling, A.L., 2016. Increasing western US forest wildfire activity: sensitivity to changes in the timing of spring. Philos. Trans. R. Soc. B 371.

Whittaker, R.H., 1960. Vegetation of the Siskiyou Mountains, Oregon and California. Ecol. Monogr. 30, 279–338.

Williams, A.P., Abatzoglou, J.T., 2016. Recent advances and remaining uncertainties in resolving past and future climate effects on global fire activity. Curr. Clim. Chang. Rep. 2, 1–14. https://doi.org/10.1007/s40641-016-0031-0.

Williams, M., Richardson, A.D., Reichstein, M., Stoy, P.C., Peylin, P., Verbeeck, H., Carvalhais, N., Jung, M., Hollinger, D.Y., Kattge, J., Leuning, R., Luo, Y., Tomelleri, E., Trudinger, C.M., Wang, Y.P., 2009. Improving land surface models with FLUXNET data. Biogeosciences 6, 1341–1359.

Williams, C.A., Vanderhoof, M.K., Khomik, M., Ghimire, B., 2014. Post-clearcut dynamics of carbon, water and energy exchanges in a midlatitude temperate, deciduous broadleaf forest environment. Glob. Chang. Biol. 20, 992–1007. https://doi.org/10.1111/gcb.12388.

Williams, C.A., Gu, H., Maclean, R., Masek, J.G., Collatz, G.J., 2016. Disturbance and the carbon balance of US forests: a quantitative review of impacts from harvests, fires, insects, and droughts. Glob. Planet. Chang. 143, 66–80.

Williams, C.A., Gu, H., Jiao, T., 2021. Climate impacts of U.S. forest loss span net warming to net cooling. Sci. Adv. 7, 1–7. https://doi.org/10.1126/sciadv.aax8859.

Yang, J., Pan, S., Dangal, S., Zhang, B., Wang, S., Tian, H., 2017. Continental-scale quantification of post-fire vegetation greenness recovery in temperate and boreal North America. Remote Sens. Environ. 199, 277–290. https://doi.org/10.1016/j.rse.2017.07.022.